We are IntechOpen, the world's leading publisher of Open Access books

Built by scientists, for scientists

6,900
Open access books available

186,000
International authors and editors

200M
Downloads

154
Countries delivered to

Our authors are among the

TOP 1%
most cited scientists

12.2%
Contributors from top 500 universities

CLARIVATE ANALYTICS
BOOK CITATION INDEX
INDEXED

WEB OF SCIENCE™

Selection of our books indexed in the Book Citation Index
in Web of Science™ Core Collection (BKCI)

Interested in publishing with us?
Contact book.department@intechopen.com

Numbers displayed above are based on latest data collected.
For more information visit www.intechopen.com

Silver Nanoparticles: Synthesis, Characterization and Applications

Neelu Chouhan

Additional information is available at the end of the chapter

http://dx.doi.org/10.5772/intechopen.75611

Abstract

Day by day augmenting importance of metal nanoparticles in the versatile fields like, catalyst, electronic, magnetic, mechanic, optical optoelectronic, materials for solar cell and fuel cell, medical, bioimaging, cosmetic, ultrafast data communication and optical data storage, etc, is increasing their value. Nanoparticles of alkali metals and noble metals (copper, silver, platinum, palladium, and gold, etc.) have a broad absorption band in the visible region of the electromagnetic spectrum of light, because the solutions of these metal nanoparticles show the intense color, which is absent in their bulk counterparts as well as their atomic level. The main cause behind this phenomenon is attributed to the collective oscillations of the free conductive electrons that are induced by an interaction with electromagnetic field. The whole incidence is known as localized surface plasmonic resonance. Out of these, we have selected the silver nanoparticles for the studies. In this article, we will discuss the synthesis, characterization, and application of the silver nanoparticles. Future prospective and challenges in the field commercialization of the nanosilver is also discussed.

Keywords: silver nanoparticles, particle size, localized surface plasmonic resonance (LSPR), characterization, application

1. Nanoparticles: an introduction

In a particle world, nanoparticles had attracted an immense attraction of the scientific world due to their large surface area to volume ratio and high reactivity with unmatchable properties. Greek Nano word used for "dwarf" means one-billionth. Nanoparticles can be served as a strong bridge between the bulk materials and atomic or molecular structures. A bulk material has constant physical properties regardless of their size and shape, but at the nanoscale, the

size, morphological substructure of the substance, and shape (as well as aspect ratios) are the major driving factors for changing their biological, chemical, and physical properties. Because at the nanoscale, the materials behave differently and they emerge with few novel characters in themselves, such as some of the materials become explosive (for example, aluminum) or their melting point changes (for example, silver and gold) or a new property is revealed (for example, nanosilver possess the antibacterial character and becomes an odor eater).

1.1. Salient features of nanomaterials

The novel properties of nano-objects occur due to the changes in size and scale. Surface area to volume ratio of the particle depends on the size and shape of an object; here, the size of the nanoparticle is very small in at least one dimension. Nanoparticles exhibited some extra phenomenon, i.e., random motion of the small particles, quantum tunneling, discreteness of energy, uncertainty of the matter, duality nature of mass, and energy for wave particles, etc. Moreover, the gravity becomes a markedly less significant force at the nanoscale, while the Vander Waals forces became incredibly strong. Therefore, the Vander Waals forces make the materials "sticky" [1]. Due to the reduction in the spatial dimension, confinement of these quasi particles in a particular crystallographic direction within a structure generally leads to changes in physical properties of the system in that direction. Some qualities (gravitational forces, vapour pressure and boiling point) of the nanoparticles decreases with their particle size and became insignificant at nanoscale because the electromagnetic force of protons is 10^{36} times stronger than gravitational forces. Here, quantum mechanics dominates in place of classical mechanics. Nanomaterials are changing their electrical, optical, surface-related, mechanical, and magnetic properties at nanoscale and exhibits some prominent effects that are associated with nanoparticles, as mentioned below.

1.1.1. Electrical properties

Because of the electrons that cannot move freely at nanolevel and their motion became restricted, this confinement at the nanoscale resulted in the changes in electrical properties, such as the bulk conductor/semiconductor materials behaving as superconductors or conductors at nanoscale. Similarly, nanogold/nanosilver (of size less than 10 nm) cannot conduct electricity.

1.1.2. Optical properties

Optical properties of nanomaterials are also size dependent. Electrons cannot move freely at the nanoscale and become restricted. The confinement of the electrons causes them to react to light differently. Gold appears golden at the macroscale, but the nanosized gold particles are red. Nanosized zinc oxide particles will not scatter visible light and bulk zinc oxide particles used for sun block as they scattered visible light and appear white. Quantum dots changes in their optical appearance as the size of the particles decreases creating different colors.

1.1.3. Surface properties

The surface-dominated properties such as melting point, rate of reaction, capillary action, and adhesion, are controlled by their surface area and due to high surface area of the nanomaterials,

these properties show drastic changes from their bulk counter parts. At the macro scale, gold has a melting point of 1064°C, but by decreasing the particle size from 100 to 10 nm diameter, its melting temperatures drops up to 100°C. As the size reduces to about 2 nm, the melting point decreases to about half of the melting point at the macroscale level [2, 3].

1.1.4. Mechanical properties

At nanolevel, the changes in mechanical properties of the material such as Young's modulus, tensile strength (four times larger), lower plastic deformation, more hardness, more brittle, grain boundaries deformations, decrease in elongation, lower density of dislocation moments, short distance of dislocation moments increases, are observed.

1.1.5. Magnetic properties

For nanomagnetic materials, each spin behaves as a small magnet for nanomaterials. The interaction between neighboring spins is dominated by the spin exchange interaction. Usually, most of the materials has $J < 0$ and are nonmagnetic (paramagnetic or diamagnetic) by nature. Similar to the paramagnets, the nanosuperparamagnets back to zero magnetization upon removing of the field. It happens because of their small size and not due to the inherently weak exchange between the individual moments.

1.1.6. Lotus effect

Lotus leaves are super hydrophobic due to high contact angle (122°) of water droplets to lotus leaf surface and presence of the needle-shaped wax tubes in these leaves, (a smaller-sized roughness region of 0.3–1.7 μm with D of 1.48) besides normal leaves pattern. Similarly, nanomaterials show the self-cleaning phenomena that are controlled by various parameters, i.e., surface fractal dimension, surface morphology, and dynamic-wetting behaviors, responsible for the super hydrophobic character in them [4].

A rough surface of lotus leaves was etched into polydimethylsiloxane (PDMS) and a negative PDMS template was made, and then, the negative template was used to make a positive PDMS reproduced as a replica sheet of the original lotus leaf. These positive PDMS templates exhibit the extreme water repellency (superhydrophobic) along with the same surface structural features as the lotus leaves shown in **Figure 1a–d** and **f**. Four classes of surfaces are revealed on the grounds of surface wettability and their contact angles are shown in **Figure 1g** [5, 6]. The chief applications of lotus effect are in making of non-wettable rain wear/sails for boats, paints for kitchen roofs/walls that make them soot-free, windows in high-rise buildings, glass for greenhouses avoiding their expensive and cumbersome cleaning, water-repellant fibers for garments, sanitary products in bathrooms/toilets and windshields motor vehicle for reducing sticking of dirt matter and easier cleaning, etc.

1.1.7. Localized surface plasmon resonance (LSPR)

When plasmonic material (nanosphere is small in comparison to the wavelength of light, and the light has a frequency close to that of the SP, then the SP will absorb energy) is exposed to
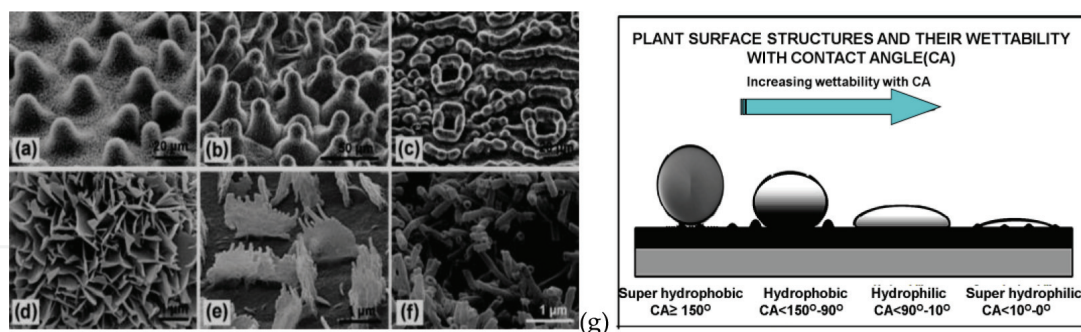
Figure 1. (a) SEM images of superhydrophobic plant leave surfaces, showing the different type of epidermal cells (a–c) and various types of epicuticular wax crystals (d–f) on leaves of *Euphorbia myrsinites* (a, d), *Xanthosoma robustum* (b, e), and *Taxus baccata* (c, f). Lotus effect associated with lotus leaves and (g) the four classes of surface wettability types of leaf surface based on their interaction with aqueous droplets [5, 6].

sunlight, free electrons of the nanoparticle of noble metals are integrated with the photon energy that produces subwaves and conducting electrons in oscillating mode [7, 8]. These collective oscillations (excitation) offer a localized surface plasmonic resonance (LSPR). LSPR adds the benefits of the enhanced local heating effect, LSPR-powered e/h generation, enhanced UV-Vis absorption, reduced e/h diffusion length, enhanced local electric effect and molecular polarization effect, quantum tunneling effect, high catalytic effect, and to the main photocatalytic unit. Hence, NPs of noble metals act as the thermal redox reaction-active centers on the catalyst that can trap, scatter, and concentrate light [9–11], and enhance the number of active sites and the rate of electron–hole formation by providing a fast lane for charge transfer on the semiconductor surface. Cu, Ag, Au, Pt, Pd, and their alloys Cu–Ag, Cu–Au, Cu–Ag–Au, are few examples of NPs of the noble metals with SPR. This phenomenon results in numerous physical effects including tailorable absorption of light (from UV to near-IR), local heating, and proficient charge transfer. Therefore, photoexcitation leads to a smooth electron transfer between the semiconductor carrier/supports and the noble-metal NPs. NPs of Ag, or Au (< 10 nm), are the most commonly used plasmonic materials.

1.1.8. The quantum confinement effect

The quantum confinement effect is observed for the particles having particle size less than the wavelength of the electron. If the motion of randomly moving electron is to be restricted in a specific energy levels (discreteness) then the motion of electron confined in three dimensions, two dimensions and one dimension, result in the particles having the shape of quantum dots, nanowire/rods and nanosheets, respectively. As the size of a particle decreases up to a nanoscale, the decrease in confining dimension makes the energy levels discrete, which widens up their band gap and band gap energy. If the size of the quantum dot is smaller than the Bohr's radius of the charge carrier (excitons, electron, hole quasi-particles of semiconductors), then the confinement observed here leads to a transition from continuous to discrete energy levels [12]. Although the physical properties of a quantum dots are not affected by quantum confinement, their optical absorption and emission can be tuned via the quantum size effect.
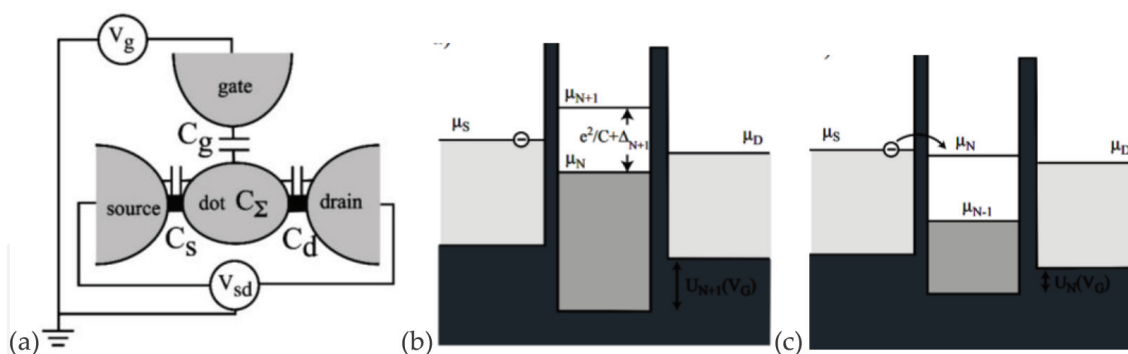
Figure 2. (a) Schematic diagram of typical arrangement of electrodes (quantum dot (QD) surrounded with source, drain and gate) for a single electron transistor. Energy diagram for a quantum dot, where the two tunnel barriers connected the QD to the source and drain contacts. (b) Electron transport is blocked and the dot contains a fixed number of N electrons. (b) Number of electrons on the QD can vary between N and N−1, result in rise a peak in the conductance because the gate voltage was tuned in order to align the chemical potential of the QD with that of source and drain [15].

1.1.9. Coulomb blockade

The phenomenon of Coulomb blockade can also be observed for a very small device (like a quantum dot) at the temperature which has to be low enough (~1 Kelvin $\cong$ 3 He refrigerators) so that the characteristic charging energy (the energy that is required to charge the junction with one elementary charge) is larger than the thermal energy of the charge carriers. But the small sized quantum dots of only few nanometers has quality to observe Coulomb Blockade from the liquid helium temperature up to room temperature (**Figures 2a–2c**) [13–15].

During the Coulomb Blockade phenomenon, the electrons inside this quantum sized device will create a strong coulomb repulsion that prevent other electrons to flow, resulting in the device will no longer follow Ohm's law as shown in **Figures 2a–2c**. When very few electrons are involved and an external static magnetic field is applied, Coulomb blockade provides the ground for spin blockade (also called Pauli blockade) and valley blockade [16, 17] which includes quantum mechanical effects due to spin and orbital interactions, respectively, between the electrons.

2. Present, past, and future of nanoparticles

History of mankind is a pursuit of color. Even in the Stone Age, people made use of pigments in paintings. In the Middle Age, the ancient Egyptians used nanotechnology but they did not understand as such in detail, but they prepared colloidal dispersion as inks and other useful products like paintings, dying hair, etc. Long ago before the beginning of the "Morden nano-era," people were well encountered with various nanosized objects and nanolevel processes, and they were using them in practice without due knowledge of the nature of these objects and processes. Thus, people were indulged in nanotechnology subconsciously, without proper understanding of the reason behind them. The secrets of nano-antiques were passed from generation to generation, without getting into the reasons behind their acquired unique

properties. Thousands of primeval knew to cultivate and process the natural fabrics, such as flax, cotton, wool, and silk, in developing the fabric of typical nanoporous materials with pores size of 1–20 nm. They were able to cultivate them and process into fine fabric product. These special fabrics possessed a developed network of pores with the size of 1–20 nm, i.e., they are typical nanoporous materials. Due to their nanoporous structure, the natural fabrics possess high-utilitarian properties as they absorb sweat well, quickly swell, and dry. Since ancient times, Egyptian people were mastered with the ways of making bread, wine, beer, cheese, and other foodstuffs, where the critical fermentation processed at nanolevel. Ph. Walter conducted a study on the hair samples from ancient Egyptian burial sites. He found that the primeval Egyptians used a nanoparticle of galenite (5 nm sized PbS) made of paste of lime, lead oxide, and small amount of water to dye hair in black. The dyeing paste reacted with sulfur of keratin, to obtain a few nanometer-sized galenite particles, to provide even and steady dyeing. The British museum possess Lycurgus Cup that was made by Roman artists in the 4th century AD, as an outstanding glass work of the primordial Rome. The impression of the Tsar of Edons (Lycurgus, **Figure 3a**) is embossed on the bowl and it shows unusual optical properties. In natural light, the bowl is green (**Figure 3b**), and if illuminated from within cup, it turns red (**Figure 3b**). The analysis of fragments of the bowl was done in 1959, by General Electric Motors for the first time, which reflected that the bowl consists of usual soda-lime-quartz glass with about 1% of gold and silver, and also 0.5% of manganese. The researchers discovered particles of gold and silver from 50 to 100 nanometers in size using an electronic microscope (**Figure 3c**), responsible for the unusual coloring of the bowl. In 2007, Harry [18] explained this phenomenon by the effects of plasmon excitation of electrons with metal nanoparticles. The Medieval Age manufacturing of multi-colored-stained glass windows (due to the gold and other metal nanoparticles) of church in Europe, are also a good example of high perfection engineering. During the battles of the European knights against Muslims, they faced the extraordinary strength of the blades of Muslims warriors in fights for the first time that was made of an ultra-strong Damascus steel (nanofibrous structure). After the discovery of electron microscopy in 1857, Michal Faraday discovered the colloidal gold in different colors: ruby, green, violet, or blue [19]. Thereafter, Albert Einstein explained the existence of colloidal dispersion in terms of Brownian motion. The above theory was experimentally confirmed by Jean-Baptize Perrin, which was awarded by Nobel Prize in 1926 [20].

Figure 3. (a) Dichroic Lycrugus cup made in 4th century AD and (b) in direct light it resembles jade with an opaque greenish-yellow tone, but when light shines through the glass (transmitted light) it turns to a translucent ruby color. (c) Transmission electron microscopy (TEM) image of a silver-gold alloy particle within the glass of the Lycurgus Cup [21].

3. Why silver nanoparticles preferred over the available nanoparticles?

Metal nanoparticles (MNPs) exhibit novel and size-related physico-chemical properties significantly different from their bulk counterpart [22]. The unique properties of MNPs have been an ambassador of their potential uses in medicine, catalysis, optics, cosmetics, renewable energies, inks, microelectronics, medical imaging, environmental remediation, and biomedical devices [23–28]. Besides, Ag-NPs exhibit a broad spectrum of bactericidal and fungicidal activity [29]. Therefore, the use of MNPs became exceptionally trendy for the wide range of consumer goods, including plastics, soaps, pastes, food, and textiles, to enhance their market value [30–32]. Among the wide range of metal nanoparticles, silver nanoparticles (Ag-NPs or nanosilver) were the most popular, due to their unique physical, chemical, and biological properties when compared to their macroscaled counterparts [33]. The advantage of the nanosilver over the other noble metals with respect to their physico-chemical properties are: small loss of the optical frequency during the surface-plasmon propagation [34], non-toxic, high electrical and thermal conductivity, stability at ambient conditions, low cost than the other noble metals such as gold and platinum, high-primitive character, wide absorption of visible and far IR region of the light, surface-enhanced Raman scattering, chemical stability, catalytic activity, and non-linear optical behavior (**Figure 4a–c**). Moreover, they exhibit a broad spectrum of high antimicrobial activity (bactericidal and fungicidal activity) attracting the scientists and technologists with much interest to develop nanosilver-based disinfectant products [35].

LSPR region of Ag, Au, and Cu in the visible and near-infrared wavelength range of sunlight is exhibited in **Figure 5a** [38]. The comparative UV/Vis diffuse-reflectance spectra of AgCl, Ag@AgCl, and N-TiO$_2$, are demonstrated by the **Figure 5b** that reflected the Ag@AgCl with plasmonic Ag molecules covers the wide range visible wavelength than other systems. The large effective scattering cross section, plasmon resonance with unique colors of the individual silver nanoparticles, as well as their non-bleaching properties have significant potential for single molecule labeling-based biological assays [40, 41]. Metal nanoparticles are also used in various near-field optical microscopic applications [42, 43] on the heels of augmented signal output due to their efficient scattering properties. Currently, nanosilver technologies have appeared in a variety of manufacturing processes and end products. There are many consumer products and applications which are utilizing nanosilver in consumer products
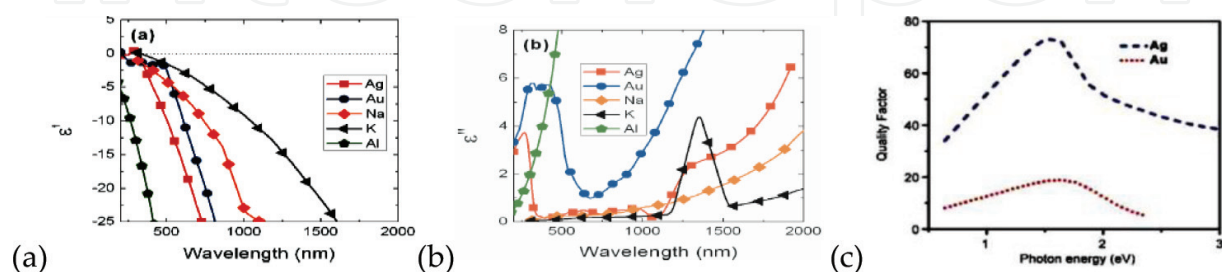

Figure 4. (a) Real and (b) imaginary part of permittivities of the metal candidates Ag, Au, Na K, and Al [36]. (c) Quality factor of plasmon resonances of a metal nanostructure as a function of plasmon frequency for two commonly used metals: silver (dashed line) and gold (dotted line) [37].
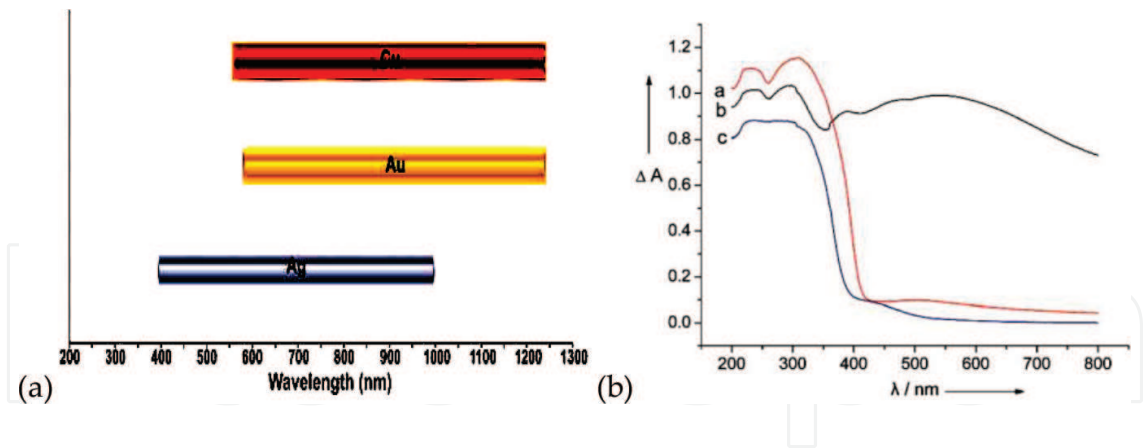
Figure 5. (a) Localized surface plasmon resonance of Ag, Au, and Cu that covers most of the visible and near-infrared wavelength range of sunlight [38]. (b) Comparative UV/Vis diffuse-reflectance spectra of (a) AgCl, (b) Ag@AgCl, and (c) N-TiO$_2$ [39].

(soap, shampoo, textile, disinfecting medical devices and home appliances to water treatments) with the highest degree of commercial value.

4. Silver nanoparticles: a plasmonic material for optical applications

During the LSPR, the light exposure in the UV-Visible wavelength range to the noble metal NPs (<10 nm), induced collective oscillations of their valence electrons [44]. The oscillating electron cloud (called localized surface plasmon/hot electrons) has the lifetime of femtoseconds order. After the lifetime, the population of hot electron started decaying via the radiative and non-radiative routes [45]. In radiative decay, they released radiations and in non-radiative decay, they were converted into photons and electron-hole pairs by inter-band/intra-band excitations that populated in conduction bands of the SP, as shown in **Figure 6**.

Surface plasmon resonance (SPR) has two different forms: (i) propagating part: surface plasmon polaritons (SPP) and (ii) stationary part: localized SPR (LSPR) [46]. The SPP traveled through resonantly excited charge oscillations on the surface of thin metal films, whereas LSPR represents
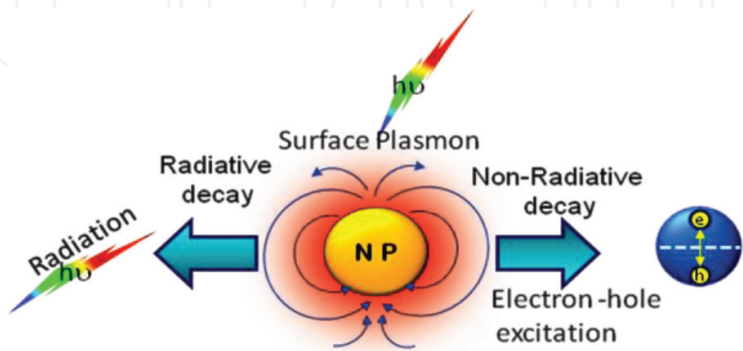

Figure 6. Schematic representation of radiative (left) and non-radiative (right) decay of the SP NP. The intra-band excitation within the conduction band results the non-radiative decay.

the non-propagating collective oscillation of the surface electrons in metal nanostructures. By utilization of SPP and LSPR in plasmonic nanostructures, the solar energy conversion efficiency of semiconductors can be improved via two paths [46]: photonic enhancement (or light trapping) and plasmonic energy transfer enhancement. In patterned plasmonic nanostructures, multiple times efficient scattering of the incident light increases the optical path length along with the light absorption direction in thin semiconductor layers [46, 47]. The previous part (SPP) contributes to enhance the energies above the band gap of a semiconductor, whereas the latter (LSPR) can induce charge separation in the semiconductor by absorbing light at the energies below the band gap [44, 48] due to the large local-field enhancement and absorption cross-section. The LSPR-induced charge separation can occur by transferring the plasmonic energy from the metal to the semiconductor via (i) direct electron transfer (DET) [49] and/or (ii) plasmon-induced resonant energy transfer (PIRET) [48]. This is referred to as plasmonic energy transfer enhancement [46] and is strong in small metal nanoparticles with small scattering cross-sections. The efficiency of the DET process depends open the relative energy of the hot electron to the height of the Schottky barrier at the interface Therefore, the semiconductor must be in close contact with the plasmonic metal. In contrast, PIRET proceeds non-radiatively based on the near-field dipole-dipole interaction between the plasmonic metal and the semiconductor [48]. PIRET allows the light absorption and the charge separation and does not require direct contact or band alignment, but its efficiency is controlled by the spectral overlap between the semiconductor's absorption band edge and the LSPR absorbance [48]. The good example of utilizing propagating (SPP) and localized (LSPR) plasmon modes is hematite nanorod array grown on a long-range-ordered plasmonic gold nanohole array pattern by combating the scattering/absorption trade-off, illustrated in **Figure 7**, where the hematite nanorods have been acted as "fiber optics miniature" to create the incarcerated modes, to trap the incident light, and to enhance the light absorption [50].

The size, shape, and composition of plasmonic NP affects the optical properties, i.e., absorption phenomena in the semiconductor, charge transport, and energetics of the semiconductor photoelectrodes as illustrated in **Figure 8** [51].
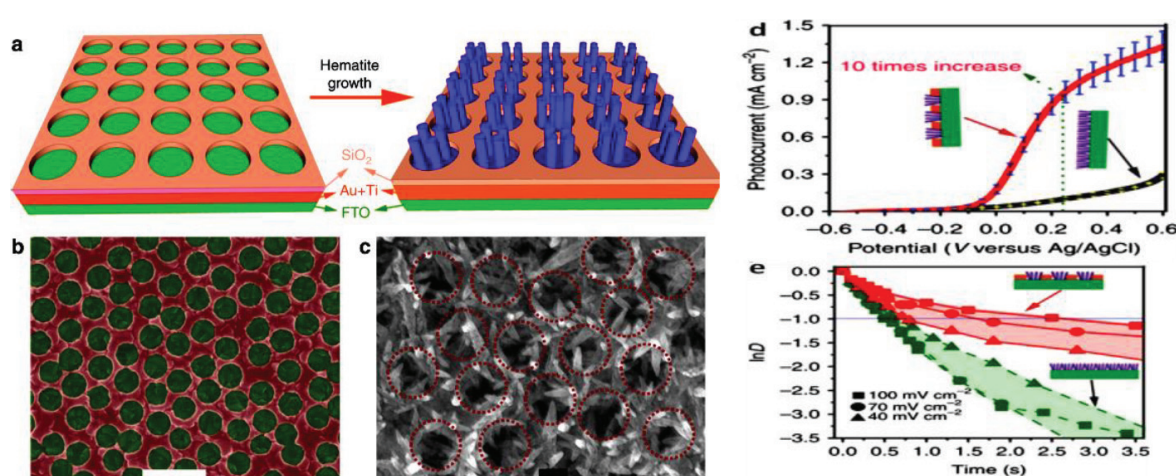

Figure 7. Architecture and microstructure of plasmonic photoanode. (a) Scheme for the growth of the hematite nanorod array on the Au nanohole array. (b, c) Scanning electron microscopic images of the Au nanohole array without (b) and with (c) the hematite nanorods. Scale bars, 1 mm (b) and 200 nm (c) [50].
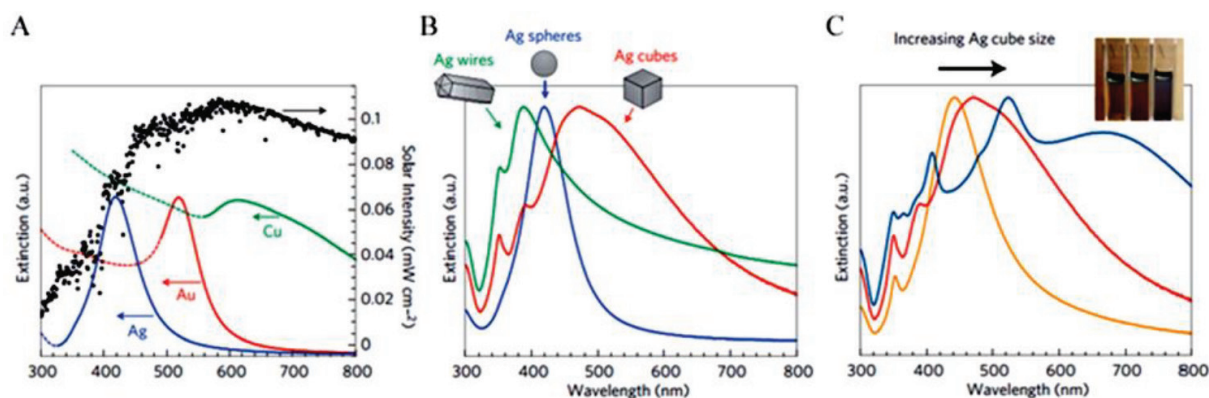
Figure 8. (A) Normalized extinction spectra of spherical Ag-NPs (38 ± 12 nm in diameter), Au NPs (25 ± 5 nm) and CuNPs (133 ± 23 nm). The solar radiation (air mass 1.5G) spectrum was taken from the National Renewable Energy Laboratory and is shown in black (http://rredc.nrel.gov/solar/spectra/am1.5/). Dashed portions of the metal extinction curves represent the inter-band transitions without surface plasmon resonance. (B) Normalized extinctions spectra of Ag-NPs with the wire (d = 90 ± 12 nm with >30 aspect ratio), cube (d = 79 ± 12 nm), and sphere (d = 38 ± 12 nm) shapes. (C) Normalized extinction spectra for Ag nanocubes as a function of size as 56 ± 8 nm (orange), 79 ± 13 nm (red), and 129 ± 7 nm (blue) edge lengths. The ethanolic suspension of the three different nanocube samples is shown in inset (reprinted with permission from Ref. [51]).

The energy of electron-electron as well as electron-phonon coupling was ultimately being converted into heat which will further thermalize the hot electrons. In the most of the cases, nonradiative (formation of electron and holes) plasmonic decay paralyzed the thermalization process that results in the efficiency minimization of the devices [52]. It not only limits the propagation length of plasmonic waveguides but also reduces the optical absorption of the metal that declines the overall performance of the device. The hot carriers generated from nonradiative plasmon decay offers new avenues to exploit the absorption losses. Although the much efforts have been devoted to alleviate the plasmon nonradiative decay, recent research has exposed the new prospectives by utilizing this energy in the areas [44, 53] such as in photothermal heat generation [45], photovoltaic devices [53, 54], photocatalysis [55, 56], driving material phase transitions [57, 58], photon energy conversion [59, 60] and photodetection [51, 61], and solar steam generation [62–64]. Most significantly, the decay of hot electrons can lead to the localized heating in the plasmonic nanostructures and making them good candidates for nanoscale heat sources [45, 65] that can be used in cancer therapy for destroying cancer cells [66]. On the contrary, hot electrons can be captured before thermalization by an adjacent semiconductor, to provide a novel photo-electrical energy conversion or chemical energy. The transformations from Plasmon energy to chemical energy occurred in four ways to drive the chemical reactions, i.e., (i) light scattering (radiative decay, **Figure 9A**), (ii) hot electron injection (HEI, **Figure 9B**), (iii) light concentration (**Figure 9C**), and (iv) Plasmon-induced resonance energy transfer (PIRET, **Figure 9D**). Light scattering by radiative decay can enhance the effective optical path length in the semiconductor. This leads to enhance the absorption of light and generation of charge carriers that can drive the chemical reactions [65].

Recently, a combination of a chiral metamaterial with hot electron injection was demonstrated in circularly polarized light detector [62, 67], where the chiral metamaterial can perfectly absorb the circularly polarized light which is the complimentary component of the largely
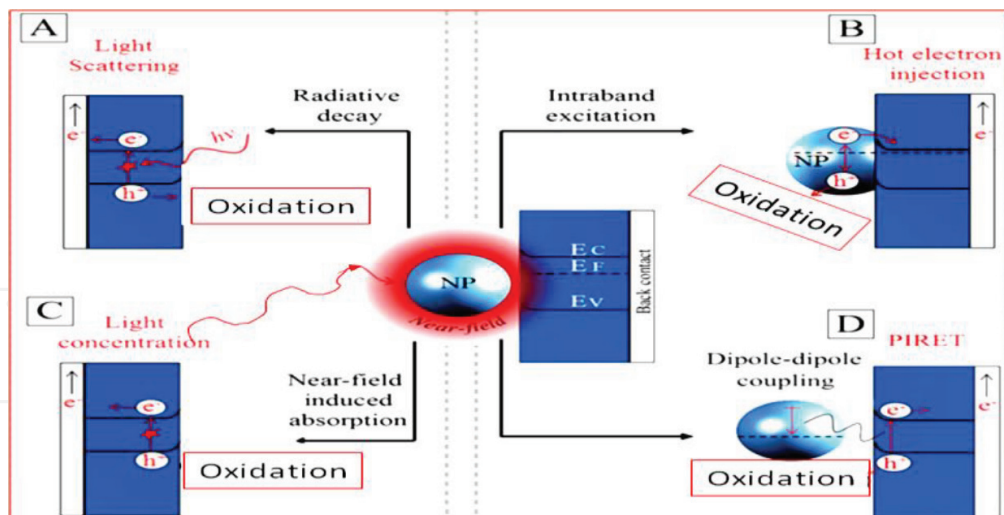
Figure 9. Schematic presentation of the transformations from Plasmon energy to chemical energy occurred in four ways (A) light scattering (radiative decay; LS), (B) hot electron injection (intra-band excitation; HEI), (C) light concentration (near field induced absorption; LC) and (D) plasmon-induced resonance energy transfer (dipole-dipole coupling; PIRET).

reflecting device. Therefore, it can be also selectively generate the hot electrons and produce a photocurrent signal depending upon the handedness of the light [62]. This ultracompact detector avoids the complexity of conventional circularly polarized light detectors, where a quarter wave-plate/polarizer were used.

In order to obtain the mechanistic insights into the structure-functionality relationship of the plasmonic NP/semiconductor composites, the decoupling of plasmon-induced and non-plasmon-induced effects are promising way to improve activity. Resonant enhancement in the polarizability of the materials with a negative real dielectric function (assuming a relatively small imaginary part) is responsible for plasmonic excitations in the metal nanoparticles.

The scattering cross section of a spherical gold NP is almost vanished when its radius decreased from 35 nm (**Figure 10A**) to 10 nm (**Figure 10B**), while the absorption and excitation
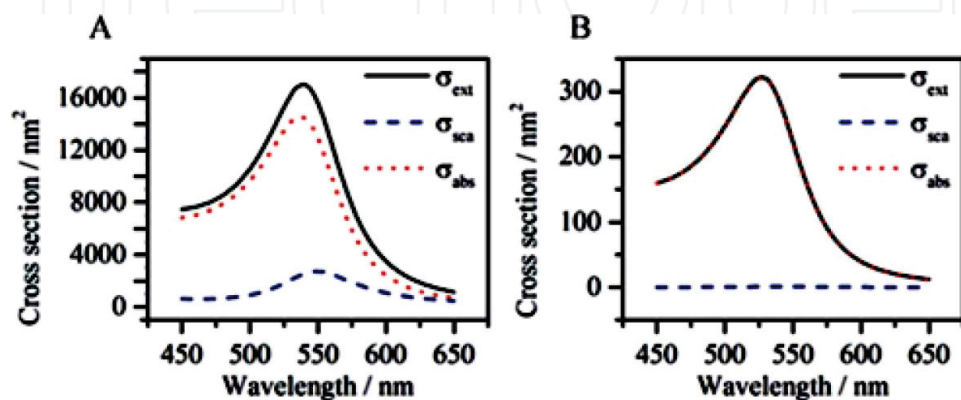

Figure 10. Extinction (black), scattering (blue) and absorption spectra (red) of a gold NP with a radius of 35 nm (A) and a radius of 10 nm (B) calculated using Mie theory. In both cases, the refractive index of the environment is 1.33 [68].

cross section are decreased to a lesser extent for the same compound. Thus, small NPs are used for applications where only non-radiative decays are desired.

5. Synthesis methods of silver nanoparticles

Recently, many techniques have been used for the synthesis of Ag-NPs by using chemical, physical, photochemical, and biological methods. Each method has its pros and cons with common problems of cost, scalability, uniform particle size, and the size distribution. Traditionally, metal nanoparticles are produced by physical methods like ion sputtering or pulsed laser ablation and chemical methods such as reduction, solvothermal synthesis, hydrothermal, sol-gel methods, and so on. However, recently, the environmentally friendly synthesis methods (by using natural products) have been developed under the branch of "green syntheses." Depending upon the selected path of synthesis and different experimental conditions, the silver NPs of different morphology, sizes, and shapes can be obtained. Nevertheless, the most important criteria is the size distribution that should be achieved as narrow as possible for the target-specific applications [69]. Four important methods (chemical, physical, photochemical, and biological) for the synthesis of nanoparticles are discussed as follows.

5.1. Chemical method

Among the existing methods, the chemical methods have been most common used for the production of Ag-NPs. The chemical reduction of metal ions is the most universal and easy route for the preparation of the metal nanoparticles. The chemical transformation of the silver ions into the silver nanostructures can occurred using photochemical method, [70, 71] wet chemical synthesis with [72] or without templates, [73] by employing liquid crystal, [74] polymer templates,[75] solution-based methodologies such as aspartate reduction [76] and starch-mediated reduction, etc [77]. Generally, the chemical synthesis process of the Ag-NPs in solution usually employs the following three main components: (i) metal precursors (for formation of AgNPs: $AgNO_3$ $AgClO_4$, $AgCl$, $(PPh_3)_3AgNO_3$, $CF3CooAg$), (ii) reducing agents, and (iii) stabilizing/capping agents. Few of the representative reducing agents are: $NaBH_4$, glucose, N,N-dimethyformamide, N_2H_4, sodium citrate, polyols, (such as ethylene glycol, diethylene glycol or a mixture of them), formaldehyde, etc., [78–83]. It is known that the different reductants are powered by different degree of reducibility that can play an important role in deciding the final shape of nanostructures. Moreover, these reductants favor the growth of nanocrystals along its different facets ((100) (111) or (110) facets). Unprotected metal colloids are highly vulnerable to the irreversible aggregation due to their small size. Therefore, the protective agents such as thiols, amines, polymers (e.g., polyvinylpyrrolidone PVP, polyvinyl alcohol PVA), polyelectrolytes (sodium oleate, oleic acid, etc.) [84–86], surfactants (cetyl trimethyl ammonium bromide (CTAB), sodium dodecyl sulfate, and cetyl trimethyl ammonium chloride (CTAC)), etc., can be added to suppression aggregation. The formation of colloidal solutions from the reduction of silver salts involves four stages, i.e., nucleation, incubation, subsequent growth, and Ostwald ripening. It is also revealed that the size and the shape of synthesized Ag-NPs are strongly

dependent on these stages. Furthermore, for the synthesis of monodispered Ag-NPs with uniform size distribution, all nuclei are required to form at the same time. In this case, all the nuclei are likely to have the same or similar size, and then they will have the same subsequent growth. The initial nucleation and the subsequent growth of initial nuclei can be controlled by adjusting the reaction parameters such as reaction temperature, pH, precursors, reduction agents, and stabilizing agents. These capping agents spontaneously adsorbed on the particle surface prevent their agglomeration, resulting in instable particle. In a typical experiment, aqueous 0.5 M $AgNO_3$ (0.8 mL) was mixed well with aqueous 0.4 M poly[(2-ethyldimethylammonioethyl methacrylate ethyl sulfate)-*co*-(1-vinylpyrrolidone)] (PQ11) (3 mL), and the resulting solution was hydrothermally treated at 100°C for 60 min. The spontaneous formation of the AgNPs can be attributed to the direct redox reaction between the PVP part of PQ11 and Ag^+, because there are no other reducing agents involved in the reaction system. As-formed dark brown colored colloidal-silver dispersion turned into yellow color (characteristic of spherical shaped AgNPs) on dilution. Usually, the bulk Ag show 4d → 5sp inter-band transitions, which are represented by the characteristic peak at 320 nm [87] in its UV-Vis spectrum (**Figure 11**). But the nano dispersion of silver display red shift and the peak at 320 nm shifted to 416 nm that corresponds to the dipole resonance of silver nanospheres.

5.1.1. Polyol process

Monodispersed solution of silver nanocubes were synthesized in large quantities by reducing silver nitrate with ethylene glycol in the presence of the capping agent polyvinylpyrrolidone (PVP) [79], which is an example of the so-called polyol process. In this case, ethylene glycol served as both reducing agent and solvent. It shows that the presence of PVP and its molar ratio relative to silver nitrate along with other additive formaldehyde, NaOH, played important roles in finalizing the geometric shape and size of the product. It suggested that it is possible to tune the size of silver nanocubes by controlling the experimental conditions.

5.1.2. Precursor injection technique

In the precursor injection method, the injection rate and the reaction temperature were important factors for producing uniform-sized Ag-NPs with a reduced size [81]. The injection of the
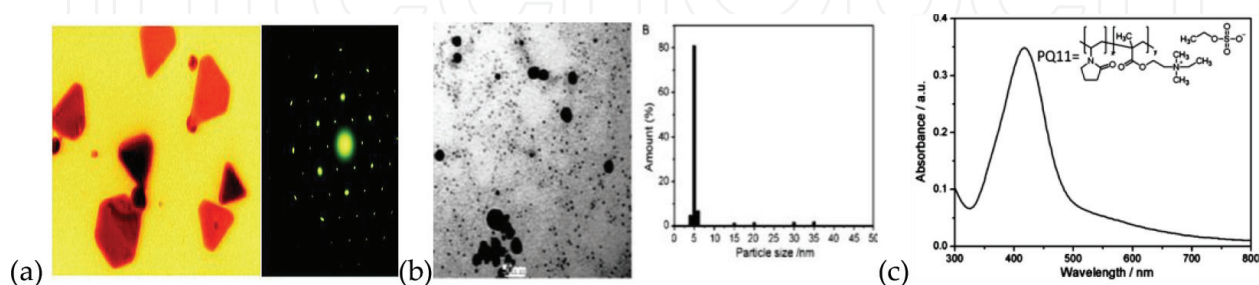

Figure 11. (a) Polygonal (mainly triangular) silver nanoprisms were synthesized by boiling $AgNO_3$ in *N, N*-dimethyl formamide and PVP, [88] (b) TEM image of as-formed silver colloids and the corresponding particle size distribution histogram and (c) UV-Vis spectrum of 150-fold diluted PQ-11 supported Ag NP solution of the dispersion synthesized at 100°C and 60min [89].

precursor solution into a hot solution is an effective mean to induce rapid nucleation in a short period of time, ensuring the fabrication of Ag-NPs with a smaller size and a narrower size distribution. Spherical Ag-NPs with a controllable size and high monodispersity were synthesized under the polyol process with the help of the modified precursor injection technique. Ag-NPs of the size 17 ± 2 nm were obtained at an injection rate of 2.5 mLs^{-1} along with the reaction temperature 100°C. Nearly, monodisperse Ag-NPs have been prepared in a simple oleylamine-liquid paraffin system [82] by using this technique.

5.2. Physical method

In the physical synthesis process of Ag-NPs, usually, the physical energies (thermal, ac power, and arc discharge) are utilized to produce Ag-NPs with a narrow size particle distribution. This approach can permit us to produce large quantities of Ag-NPs samples in a single process. Under the physical methods, the metallic NPs can be generally fabricated by evaporation-condensation process that could be carried out in a tube furnace at atmospheric pressure. The large space of tube furnace, consumption of large amount of energy, raising the environmental temperature around the source material and a lot of time for achieving thermal stability, are the few drawbacks of the method. Another physical method of synthesis of Ag-NPs is a thermal decomposition method that used to synthesize the powdered Ag-NPs [90]. In particular case, Ag-NPs (particles with particle size of 9.5 nm with a standard deviation of 0.7 nm) were formed by thermal decomposition of a Ag^{1+}–oleate complex, at high temperature of 290°C. This indicates that the Ag-NPs were prepared with a very narrow size distribution. Jung et al. [91] reported a small ceramic heater (with a local heating area) for synthesizing the metal NPs and by evaporating the source materials under the flow of carrier gas, i.e., air. It had been reported that the geometric mean diameter, the geometric standard deviation, and the total concentration of spherical NPs without agglomeration increases with the temperature of the surface of the heater. The testimony given by Tien et al. [92] reveal the fabrication technique for the Ag-NPs by employing the electrical discharge machining (EDM) without addition of any surfactants. Where, pure silver wires were submerged in deionized water and treated as electrodes. The stability of suspension, concentration of particles, particle size, solution properties, electric conductivity, and pH are the factors that may affect the synthesis of NPs by enhancing the complex interactions to the nanofluid, in the form of van der Waals combination force and electrostatic Coulomb repulsion force. Metallic Ag-NPs of the 10 nm size and ionic silver of approximate concentrations 11–19 ppm were obtained by silver rod at the consumption rate ~ 100mgmin^{-1}. More recently, Siegel et al. [93] reported an unconventional approach for the physical synthesis of gold-NPs and Ag-NPs by the direct metal sputtering into the liquid medium (glycerol-to-water).

5.3. Photochemical synthesis

The photo-induced synthesis of Ag-NPs has two main approaches: that is the photophysical (top down) and photochemical (bottom up) ones. In former way, NPs could be prepared by the fragmentation of the bulk metals and followed by generation of the NPs from ionic

precursors. The NPs are formed by the direct photoreduction of a metal ion using photo-chemically generated intermediates, such as excited molecules and radicals, which are often known as photosensitization of NPs [94, 95]. The main advantages of the photo-induced process are: clean process, high spatial resolution, convenience of use, the controllable in-situ reducing agents generation; the formation of NPs can be triggered by the photo irradiation, (iii) enables one to fabricate the NPs in various mediums including emulsion, surfactant micelles, polymer films, glasses, cells, etc [94]. The direct photo-reduction process of $AgNO_3$ takes place in the presence of sodium citrate (NaCit) using different light thermal sources (UV, white, blue, cyan, green, and orange) at room temperature [96]. This light-induced process results in a metallic colloid with size and shape powered distinctive optical properties of the particles. Reproducible UV photo-activation method is used for the preparation of the stable Ag-NPs in aqueous TritonX-100 (TX-100) [97], where TX-100 molecules play a dual role: (i) as an reducing agent and (ii) as a NPs stabilizer through template/capping action. The addition of surfactant solution to TX-100 and silver precursor helps in carrying out the NPs growth process by controlling the diffusion (by decreasing the diffusion/mass transfer coeffi-cient of the system) to improve the NPs size distributions (by increasing the surface tension at the solvent–NPs interface). The Ag-NPs (size 2–8 nm) can also be synthesized in a basic aqueous $AgNO_3$ solution and carboxymethylated chitosan (CMCTS) under UV light irradia-tion. CMCTS is a biocompatible water-soluble derivative of chitosan and served as a reducing agent for silver cation and a stabilizing agent for Ag-NPs (stable for more than 6 months), simultaneously [98]. This method is used to fabricate a high-yield metal nanostructures and composite materials at low cost. Few alternative approaches, such as laser ablation at the solid–liquid interface and combination of the reducing agent and sunlight, are also used for metal nanostructure fabrication. The three-dimensional metal NPs are produced using laser ablation and are applicable in the field of a light-driven actuator, bioimaging, and three-dimensional processing [99]. The photo-induced silver nanoprisms/nanodecahedrons have been the synthesis by controlling the concentration of sodium citrate and sunlight (ultraviolet light). At the lower concentration of citrate ($\leqslant 5.0 \times 10^{-4}$ M), silver nanoprisms are converted into nanodecahedrons silver by increasing the concentration of citrate as shown in **Figure 12**. Although the intensity of light affects the shape of the NPs, the lighting power density did not influence the shape conversion except for reaction rate [100].
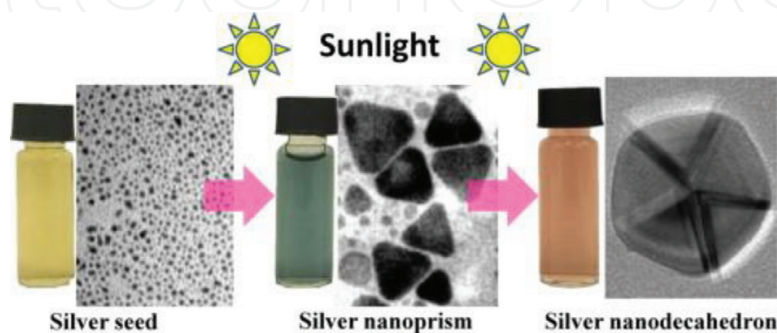

Figure 12. Photo-induced synthesis of silver nanoprisms and nanodecahedrons by controlling the concentration of sodium citrate and sunlight [100].

5.4. Biological synthesis

Usually, wet-chemical or physical method is used to prepare the metal nanoparticles. However, the chemicals used in pbhysical and chemical methods are generally expensive, harmful and inflammable but the bogenic methods are a cost effective, energy saver and having enviornmentally benign protocols technique for green synthesis of silver nanoparticles from different microorganisms (yeast, fungi and bacteria, etc) and plant tissues (leaves, fruit, latex, peel, flower, root, stem, etc) as shown in **Figure 13**. Pytochemicals (lipids, protiens, polyphenols, carboxylic acids, saponins, aminoacids, polysachccarides amino cellulose, enzymes, etc.) present in plants are used as reducing and capping agent. The use of agro waste and micro-orgamisms materials not only reduces the cost of synthesis but also minimizes the need of using hazardous chemicals and stimulates "green synthesis" way for synthesizing nanoparticles [101, 102].

This method of biosynthesis is very simple, requiring less time and energy in comparison to the physical and chemical methods with predictable mechanisms. The other advantages of biological methods are the availability of a vast array of biological resources, a decreased time requirement, high density, stability, and the ready-to-soluble as-prepared nanoparticles in water [103]. Therefore, biogenic synthesis of metal NPs unwraps up enomorus opportunities for the use of biodegradable or waste materials.
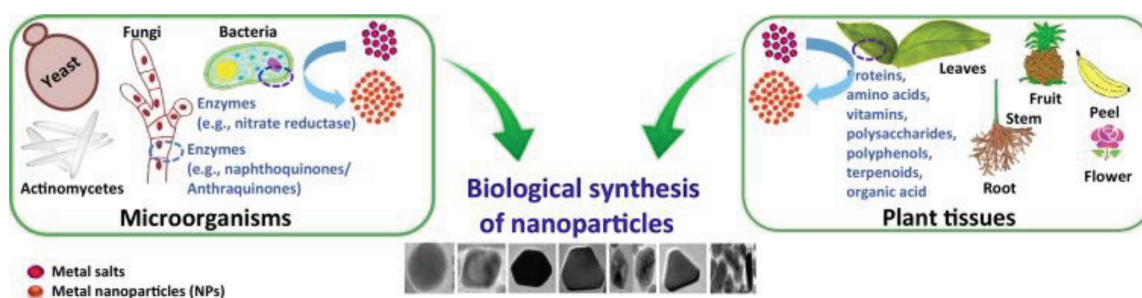

Figure 13. Biogenic synthesis of metal nanoparticle of various shape and size using microorganisms and plant tissues extracts.

6. Characterization tools for analysis of silver nanoparticles

At the nanoscale, particle-particle interactions are either dominated by weak Vander Waals forces, stronger polar and electrostatic interactions or covalent interactions. Characterization of nanoparticles is vital part of determination of the phase purity, shape, size, morphology, electronic transition plasmonic character, atomic environment and surface charge, etc. By using advanced analytical techniques such as electron microscopic techniques (atomic force microscopy (AFM), electron energy loss spectroscopy (EELS), surface enhanced Raman scattering (SERS), scanning electron microscopy (SEM) and transmission electron microscopy (TEM) and their corresponding energy-dispersive X-ray spectroscopy (EDX), and selected area electron diffraction (SAED for crystallinity). Properties like surface morphology, size, and overall shape are determined by electron microscopy techniques and

elemental composition by SEM-/TEM-/EELS-supported EDX. Optical analysis techniques such as Fourier transform infrared (FTIR) spectroscopy, fluorescence correlation spectroscopy (FCS, diffusion coefficients, hydrodynamic radii, average concentrations, and kinetic chemical reaction), X-ray diffraction (XRD for phase purity with crystal parameters and particle size), diffuse light scattering (DLS can probe the size distribution of small particles), UV-Vis spectroscopy (band gap, particle size electronic interaction), XPS (X-ray photon spectroscopy, surface environment of elemental arrangement), Raman spectroscopy (it provides submicron spatial resolution average size and size distribution through analysis of the spectral line broadening and shift), nuclear magnetic resonance (NMR can detect structure, compositions, diffusivity of nanomaterials, dynamic interaction of species under investigation), small-angle X-ray scattering (SAXS; from 0.1° to 3° can evaluate the size distribution, shape, orientation, and structure of a variety of polymers and nanomaterials), zeta potential with a value of ±30 mV is generally chosen to infer particle stability. Above analysis can be used to determine the properties of nanomaterials such as the size distribution, dispersibility, average particle diameter, charge affect the physical stability and the in vivo distribution of the nanoparticles. Few of above are discussed below.

6.1. X-ray diffraction spectroscopy (XRD)

The crystalline structure, size, and shape of the unit cell and the crystallite size of a material can be determined using X-ray diffraction spectroscopy (XRD). Usually, X-ray diffraction peaks were observed at 2θ = 38.00°, 44.16°, 64.40°, and 77.33°, which correspond to (111), (200), (220), and (311) Bragg's reflections of the face-centered cubic (fcc) structure of metallic silver, respectively (standard JCPDS card No. 04-0783 or 87-0597). The crystalline size of the particulate can be estimated by using the Debye-Scherrer formula d = 0.89λ βcosθ, where d is the particle size, λ is the wavelength of X-ray radiation (1.5406 Å), β is the full-width at half-maxima (FWHM) of the strongest peak (in radians) of the diffraction pattern and 2θ is the Bragg angle [104].

6.2. Scanning electron microscopy (SEM)

In this technique the whole sample is analyzed by scanning with a focused fine beam of electrons and electrostatic or electromagnetic lenses to generate images of much higher resolution. Surface morphology of the sample is determined by the help of the secondary electrons emitted from the sample surface.

6.3. Transmission electron microscope (TEM)

In TEM analysis, an incident beam of electrons is transmitted through an ultra-thin sample which interacts with the sample and transforms into unscattered electrons, elastically scattered electrons, or inelastically scattered electrons. The scattered or unscattered electrons are focused by a series of electromagnetic lenses and then projected on a screen to generate a electron diffraction, amplitude-contrast image, a phase-contrast image, or a shadow image of varying darkness according to the density of unscattered electron. Transmission electron microscopy

techniques can provide direct imaging, diffraction and spectroscopic information, chemical composition, either simultaneously or in a serial manner, of the specimen with an atomic or a sub-nanometer spatial resolution. High-resolution TEM imaging, when combined with nanodiffraction, scanning tunneling microscopy (STM), atomic resolution electron energy-loss spectroscopy, and nanometer resolution X-ray energy dispersive spectroscopy techniques, is critical to the fundamental studies of importance to nanoscience and nanotechnology.

Different surface structures can be obtained from various synthesis routes. Surface morphology of the nano-structural features of silver are examined using above electron microscopic techniques. Electron microscopy images of single-crystal Ag-NPs (cubes, bars, wires, and bipyramids) grown in ethylene glycol in the presence of PVP and Br− at different proportions, are demonstrated in the **Figure 14A–D**. Silver triangular nanoplates, prepared by are demonstrated by the **Figure 14E** and **F** Asymmetric Silver "Nanocarrot" Structures, were synthesized by using wet chemical method using CF3COOAg as precursor, PEG as reducing agent, and PVP as capping agent are depicted in the **Figure 14G–I** [105, 106].

6.4. Scanning tunneling microscopy (STM)

STM uses quantum tunneling current to generate electron density images at the atomic scale for conductive/semiconductive surfaces and biomolecules attached on conductive substrates [107]. A sharp scanning tip, an xyz-piezo scanner controlling the lateral and vertical movement of the tip, a coarse control unit positioning the tip close to the sample within the tunneling range, a vibration isolation stage and feedback regulation electronics are the basic parts of the STM instrumentation. Its working on the generic principle for, i.e., to bring a susceptible probe in close proximity to the surface of an object measured to monitor the reactions of the probe [108].

6.5. Atomic force microscopy (AFM)

The AFM can investigate the size, shape, structure, sorption, dispersion, and aggregation of nanomaterials. It is based on a physical scanning of samples at sub-micron level (contact or noncontact mode) using a probe tip of atomic scale and offers ultra-high resolution (>100 times
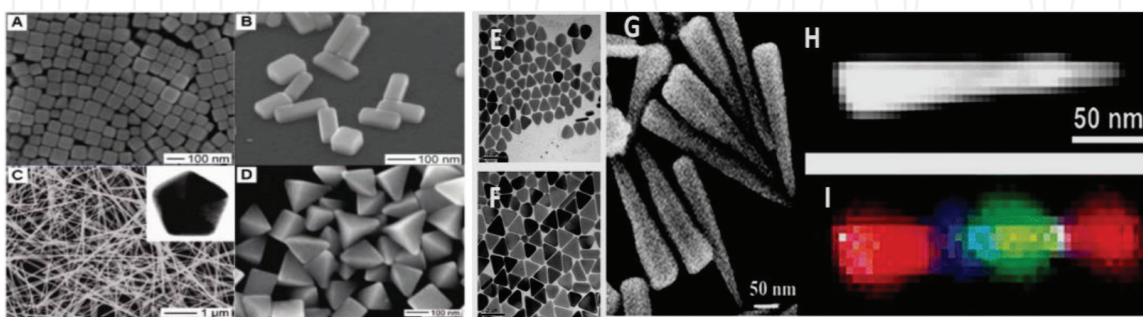

Figure 14. Electron microscopy images of single-crystal Ag nanocrystals: (A) nanocubes prepared in ethylene glycol with PVP as a capping agent in DMF; (B) nanobars prepared in ethylene glycol in the presence of PVP and Br−; (C) pentagonal nanowires prepared in ethylene glycol in the presence of PVP in DMF; (D) bipyramids prepared in ethylene glycol in the presence of PVP, where TEM image represented by E, F, and G and the EELS spectrum of the asymmetric silver nanocarrot, were represented by H&I [105, 106].

better than the optical diffraction) in particle size measurement. One of the principal advantages of this nondestructive technique is that it felicitates the imaging of the non-conducting samples without any specific pretreatment and without causing appreciable harm to the surface. The major drawbacks of this technique is (i) the size of the cantilever tip is generally larger than the dimensions of the nanomaterials to be examined that led to unfavorable overestimation of the lateral dimensions of the samples [109, 110], (ii) AFM also lacks the capability of the detecting or locating specific molecules; however, this disadvantage has been eliminated by recent progress in single-molecule force spectroscopy with an AFM cantilever tip carrying a ligand.

6.6. Electron energy-loss spectroscopy (EELS)

In looking to the better understanding of the atomic processes in solids, their emerging demand for new imaging, diffraction and spectroscopy methods with high-spatial resolution. That demand has been reinforced by the growing interest of human being in nanomaterials. Although, the transmission electron microscopy (TEM) can provide the structural information with excellent spatial resolution (down to atomic dimensions) through high-resolution TEM imaging and electron diffraction technique, electron energy-loss spectroscopy offers unique possibilities for the nanoscale thin materials (plasmonic) analysis. Due to the broad range of inelastic interactions of the high energy electrons with the specimen atoms, ranging from phonon interactions to ionization processes, EELS and their combination with TEM offers the facility to map the elemental composition of a specimen for studying the physical and chemical properties of a wide range of biological and non-biological materials. Moreover, the energy distribution of all the inelastically scattered electrons provides the information [111] about the local environment of the atomic electrons for the universal dispersions of surface plasmons in flat nanostructures, [112] 3D distribution of the surface plasmons around a metal nanoparticle [113] and exotic nanostructures are shown in **Figure 15** [114].

6.7. UV-Visible spectroscopy analysis

In decades past, synthesis of silver nanostructures has been an active research area because of their excellent optical properties such as surface-enhanced Raman scattering (SERS) and

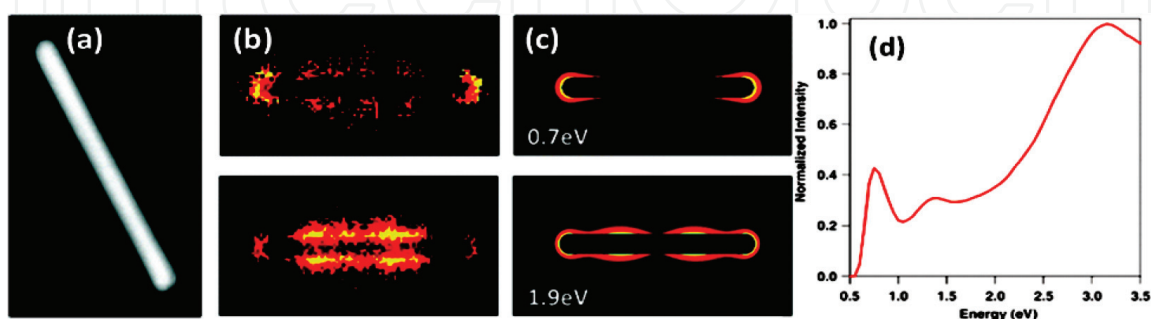**Figure 15.** EELS data and corresponding electrodynamic calculation for rod. (a) Annular dark field (ADF) image of rod with high aspect ratio 9.6, (b) multivariate statistical analysis (MVSA)) score images, (c) discrete dipole approximation (DDA) calculated electric field plots displaying the field generated by a plane wave optical excitation at the energies and polarization given on each plane, and (d) summed EEL spectrum [114].

surface plasmonic resonance, which strongly depend on size, shape, and composition, and can be checked by the help of the optical analyses like XPS and UV-Visible spectroscopy analysis. Although, the change in color of precursor silver ion to silver nanoparticles was visually observed, the absorption measurements were carried out using UV-Visible spectrophotometer to check the stability of silver nanoparticles. Characteristic UV-Vis spectrum peak of bulk Ag appears at 320 nm due to the inter-band $4d \rightarrow 5sp$ transitions [87]; and the red shift in this peak to around 420 nm was observed due to the occurring of the plasmonic resonance phenomenon in the nano-dispersion of silver metal. Effect of shape and size on optical properties of the silver nanoparticle is reflected by **Figure 16**.

UV-Vis spectroscopy also used for particle size determination of silver nanoparticles, using Mie scattering theory. The full width at half maxima of the optical spectra (Lorentz-shaped peak; Ω) can be used to calculate the particle size of stable suspension by using following equation [116, 117]:

$$D = \frac{(\epsilon_0 + 2n^2)\, c\, m\, U_F}{2N_c e^2 \omega} \tag{1}$$

where, w is full width at half maxima of the Lorentz shaped peak, and ϵ_0, n, c, m, U_F, N_c, e, and D, are the frequency independent dielectric constant, refractive index of water, velocity of light, mass of electron, electron velocity at the Fermi energy, number of electrons per unit volume, the electron charge and diameter of the particle, respectively.

6.8. Surface-enhanced Raman scattering spectroscopy (SERS)

SERS can be employed as a sensitive and selective technique for identification of molecules. Strong electromagnetic fields are generated due to the localized surface plasmon resonance (LSPR) of nano-noble metals, when they are exposed to visible light. If the Raman scatterer is placed near these intensified electromagnetic fields of nano-noble metals, the induced-dipole

Figure 16. (a) optical spectra of the individual silver nanoparticles of different shape spherical (Blue emission), pentagon (Green emission) and triangular (Red emission) as reflected from their typical high resolution TEM images. (b) Plot of the lateral size of TEM images vs the wavelength of the plasmonic resonance spectral peak for a spherical (dark circle; 85%) pentagon (empty rectangle; 5%) and triangular (dark triangle; 5%) particles [115].
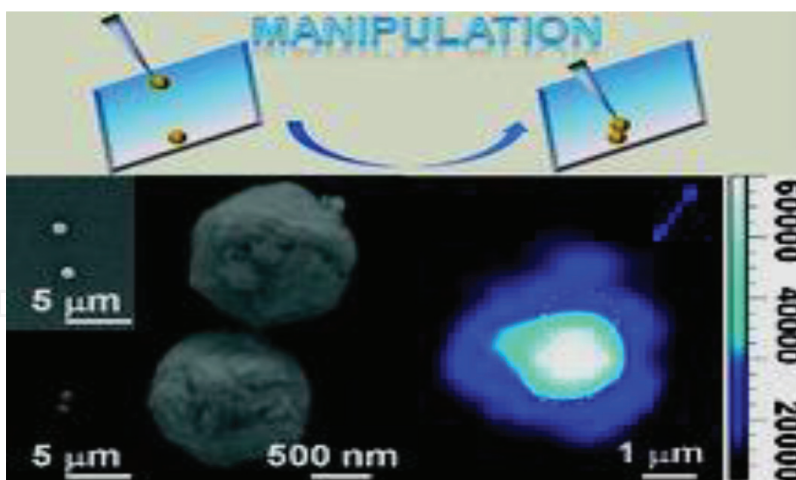
Figure 17. SEM images of a self-assembled dimmer of flower-like silver mesoparticles along with their corresponding Raman images at the axis parallel to the dimer axis of the detected particles with high SERS quality [118].

increases that results in the increase of intensity of the inelastic scattering. Similar relations can hold-good for the extinction and scattering cross sections of the nanoparticle. If the extinction and scattering cross sections of the nanoparticle at resonant wavelengths are maximized, it represents the spectroscopic signature of exciting the LSPR. A SER spectrum also provides the accurate information about molecular structure and the local environment in condensed phases than any other electronic spectroscopy technique.

A typical example of the surface-enhanced Raman scattering (SERS) is reflected by **Figure 17**, where the coupling effect still dominates the SERS and the flower-like silver mesoparticle dimer image with the large hot areas is ≈10 to 100 times greater than the individual mesoparticles [118].

7. Applications of the silver nanoparticles

Metal nanocatalysts of different shapes and sizes like quantum dots, nanotubes, nanofibres, nanolithographs, self-assemble processing devices, nanoparticles, and nanofibres, have immense significance. They have bright future in broad research areas of high-tech applications in the field of information of storage, computing, medical and biotechnology, energy, sensors, photonics, communication, and smart materials. The size and shape of the nanometal is a critical criteria to target-specific applications that may be achieved by keeping size distribution as narrow as possible. Nanometals has enormous potential to serve all facets of life for building big future from small things, as they acquire the goodness of both homogeneous and heterogeneous catalysts. At present, the pretty command over the morphologies of silver nanoparticles has received immense attention of researchers due to their considerable budding applications in almost all fields. In the present context, they have attracted the interest of the people due to their unique physical, chemical, and biological properties in compared to their massive counterparts. Silver nanoparticles are also studied by material scientists who investigate their integration into other materials in order to obtain enhanced properties, for example, in solar cells where silver

nanoparticles are used as plasmonic light traps. These properties make them valuable in other applications such as catalyst [119, 120], inks, microelectronics, medical, imaging, health products, and waste management. Antifungicidal activities making them extremely popular in a diverse range of consumer/medical products, including plastics, soaps, pastes, food, cosmetics, medicine, highly sensitive surface-enhanced Raman spectroscopy (SERS) application [121–123], water treatment and textiles, etc., that boost their market value [124]. Moreover, the nanofibre can be very effective in attracting and trapping small particles because it is "sticky" due to its large surface area. This makes nanofibres excellent materials for use in filtration [125]. Moreover, silver nanoparticles accounts for more than 23% of available nano-products in the market. It includes the share of different facets of life, i.e., 52.61% health and fitness, 10.44% cleaning, 10.04% food, 6.02% household equipments, 4.02% medicine, 3.21% electronic devices, 2.01% toys, and 11.65% others [126]. Out of the versatile applications of nanosilver in diverse phases of life, few are discussed below.

7.1. Medical: diagnosis and treatment of aliment

The silver nanoparticles exhibit a broad spectrum of antibactericidal, antiviral, anti-inflmmatory, antiangiogenic, anti-tumor, and anti-oxidativeproperties along with the biological and chemical sensing, imaging, drug carrier, and diagnosis of the cancer/HIV/AIDS [127–131]. When the researchers directed near-infrared laser light through the mice's skin and at the tumors, the resonant absorption of energy in the embedded nanoshells raised the temperature of the cancerous tissues from about 37°C to about 45°C. The photothermal heating killed the cancer cells while leaving the surrounding healthy tissue unharmed. In the mice treated with nanoshells, all signs of cancer disappeared within 10 days; in the control groups, the tumors continued to grow rapidly [132].

Silver nanotechnology, emerging as a fast growing technology in the field of orthopedics due to its antimicrobial properties. Therefore, silver nanoparticles can be used in orthopedic applications such as trauma implants, tumor prostheses, bone cement, and hydroxyapatite coatings to prevent the biofilm formation. Bio film formation is a major source of morbidity in orthopedic surgery. The promising results with *in vitro* and *in vivo* studies of the use of AgNPs in this field reduce the risk of infection in an effective and biocompatible manner [133].

7.2. Food industry

Silver nanoparticles are already utilized for various applications in areas such as food supplements, food packaging, and functional food ingredients. To protect the food from dust, gases (O_2, CO_2), light, pathogens, moisture nanocomposite LDPE films containing Ag and ZnO nanoparticles packaging, would be a safer, inert; cheaper to produce, easy to dispose and reuse-way. Nanocomposite LDPE films containing Ag and ZnO nanoparticles were prepared by melt mixing in a twin screw extruder. Packages prepared from the above films were used to carry/ store fresh orange juice, fresh meat (highly perishable commodity) to avoid the proliferation of undesirable microorganisms and also to provide desired texture to the food, encapsulate food components (e.g., control the release of flavors), increase the bioavailability of nutritional components [134].

7.3. Catalyst

In recent years, one of the most important applications of the AgNPs has been observed in catalysis of chemical reactions. Nanosilver catalysts' with their unique reactivity and selectivity, stability, as well as recyclability in catalytic reactions with atom-economy and environmental benign nature, increases the interest in nanosilver-mediated organic synthesis in the last few years. Nanosilver of different shapes and sizes catalyzed many organic transformations such as cyclization, Michael addition, alkylation, alkynylation, oxidation, cross-coupling reaction, A^3-coupling reaction, reduction, Friedal-crafts, Diel-Alder reaction, and many more [135]. Researchers are fascinated to silver nanoparticles, since it has enabled unprecedented or low selective transformations to highly reactive and chemoselective catalysis for various nanosilver-catalyzed reactions. For example, kinetically difficult reduction of p-nitrophenol is not possible even in presence of strong reducing agent $NaBH_4$ and month long aging. But, by the addition of AgNPs in the same reaction mixture, it made the reaction possible by formation of the p-aminophenol [136]. Studies in this field, revealed the strong potential of nanosilver catalysis in the total synthesis of natural products and pharmaceutical molecules [137].

7.4. Air disinfection (biosols filter)

Bioaerosols are airborne biological origins such as viruses, bacteria, fungi, which are capable of causing infectious, allergenic, or toxigenic diseases. Large quantities of these bioaerosols were accumulated on the filters of heating, ventilating, and air-conditioning (HVAC) systems [138]. It often resulted in the low quality of indoor air. The WHO estimated that 50% of the biological contamination present in indoor air comes from filter-medium after air filtration, which can add on microbial growth. These pathogens generate mycotoxins which are dangerous to human health. To reduce the microbial growth in air filters, Ag-deposited-activated carbon filters (ACF) were effectively used for the removal of bioaerosols. Antibacterial activity analysis of Ag-coated ACF filters was checked for *Bacillus subtilis* and *E. coli* [138]. It was found that above two bacteria were completely inhibited the physical properties of ACF filters such as pressure drop and filtration efficiency with in 10 and 60 min, respectively.

7.5. Drinking water purification

Studies supported that the silver nanoparticle (AgNP) can work as an excellent antiviral, antimicrobial, and disinfectant agents. The results obtained showed that silver nanoparticles in surface water, ground water, and brackish water are stable. However, in seawater conditions, AgNP tend to aggregate. The comparison of AgNP-impregnated ceramic water filters and ceramic filters impregnated with silver nitrate was made. The results showed that AgNP-impregnated ceramic water filters are more appropriate for this application due to the lesser amount of silver desorbed compared with silver nitrate-treated filters without disturbing the water chemistry conditions and performance of the filters. Quaternary ammonium functionalized silsesquioxanes-treated ceramic water filter desorbed less from the filters and achieved higher bacteria removal than the filters impregnated with AgNP. This indicates that

the quaternary ammonium functionalized silsesquioxanes compound could be considered as a substitute for silver nanoparticles due to its lower price and higher performance [139].

7.6. General/health care

Nanosilver products such as beauty soap, hair shampoo and conditioner, body cleanser, tooth brush, sanitizer, facial masksheets, skin care line, makeupline, wetwipes, disinfectant spray, wash and laundry detergent, etc., have been influence our daily life at great extent [140]. Silver nanoparticles can also be incorporated in manufacturing of the toothpaste or oral care gels. Silver nanoparticles with particle size less than 15 nm and concentration of 0.004% w/w showed maximum efficiency to prevent the growth of bacteria that causes unpleasant oral smells and dental cavities [141].

The nanoproduct can also be used in dyeing of cosmetic foundations, eye shadows, powders, lipsticks, inks, varnishes, or eyebrow pencils. According to Ha et al., the products with metal nanoparticles, unlike the conventionally used metallic pigments, are not harmful to human health, and may even have health benefits [142].

A soap with silver nanoparticles as one of the ingredients was prepared; and in 2013, the method for its preparation was patented [143]. Nia had used the silver nanoparticles to improve the plant growth of the plants (citrus fruits, grains, and oleaceae trees) [144]. Silver nanoparticles-treated structure of textile materials [145] were used for antimicrobal activities protected clothing. The authors reported that the silver nanoparticles coated nylon fibers used in making of floor coverings/carpets that helps to secure them against bad odors and the growth of pathogenic microorganisms [146].

8. Challenges and perspectives

The commercial use of the engineered nanomaterials, with at least one-dimension of 100 nm or less, is increasing in the area of fillers, opacifiers, consumer/medical products (including plastics, soaps, pastes, food, cosmetics, medicine, drug carriers, and highly sensitive SERS application), catalysts, semiconductors, textile, waste water treatment, microelectronics, bioimaging, etc. Materials at nano-level may induce some specific physical or chemical interactions with their environment. As a result, they perform exceptional changes in the properties like conductivity, reactivity, and optical sensitivity, in comparison to their massive counterparts, which may enhance the processes such as dissolution, redox reactions, or the generation of reactive oxygen species (ROS). These processes may be accompanied by biological effects that would not be produced by larger particles of the same chemical composition. The nanomaterials are responsible for the possible undesirable interactions with biological systems and the environment which might generate toxicity. Therefore, there is an urgent requirement to establish the principles, procure the test procedures to ensure safe manufacture and commercial use of nanomaterials [147] to stop the uncontrolled release of nanoparticles to the environment through waste disposal, and to incorporate the nanowaste and nanotoxicology in the waste management. Thus, the bioaccumulation and toxicity of the nanoparticles may

become important environmental issues. Although the amount of the nanoparticles in commercial products are lower than those present in soluble form but the toxicity resulting from their intrinsic nature (e.g., their size, shape, or density) may be significant. Moreover, the major challenge in the treatment of nanowaste is the current need of the time. Not only the proper understanding of its chemical, physical, and biological properties, but it also requires the apt number of studies on the impact (short- and long term effects) of these new materials on biological and environmental systems (acutely lacking area). It is necessary to have basic information from companies about the level and nature of nanomaterials produced or emitted and about the expectation of the life cycle time of nanoproducts as a basis to estimate the level of nanowaste in the future. Without the knowledge of how to use, store, facilitate the separation, and recovery of recyclable and non-recyclable nanomaterials, the development of the regulations in this field is difficult. Moreover, Ag metal has strong affinity toward the elements, i.e., O, Cl, S, and organic compounds (particularly, the thiol group containing compound) and oxidation capacity that shorten the lifetime of Ag-NPs in the environment. The kinetics of Ag-NPs corrosion increases with decreases in particle size. Sulfidation (significant amount of the sulfide ion present in polluted water) is the most probable corrosion process for metallic AgNPs undergo because of the very high stability of Ag_2S. However, the mechanisms with the kinetics of the oxidation of Ag_2S-NPs in to Ag_2SO_4, on contact with air or microbial transformation, is needed to be deal with as Ag_2SO_4 (Ksp = 1.2×10^{-5}) is considerably more soluble than Ag_2S (Ksp = 5.92×10^{-51}). Furthermore, in comparison to the unsulfidized AgNPs and Ag ion, the toxicity of Ag_2S-NPs has shown limited acute toxicity because sulfidation momentously decreases the solubility [148]. Recently, the plasmonic materials are in fashion because of their efficiency in optoelectronic materials; for example, in a recent report, the hot electron transfer from a plasmon-induced interfacial charge-transfer transition induced the quantum efficiency of the device up to 20% independent of incident photon energy [149]. In addition to above, a better understanding of the hot carrier generation, transport, emission and relaxation timescale, engineering of semiconductor-hot electron interface is still needed for better designing of the efficient hot carrier devices [150–153]. Beside all the challenges, the future of silver nanoparticles is bright because of their potential use in biomedical applications as long lasting and enhanced antifungal, antibacterial, disinfection properties along with their utilization in drug delivery, diagnosis, bioimaging, biosensing, etc. Moreover, their role as an effective molecular sieve, metallic sorbent, and catalyst for the removal of the environmental pollutions are commendable. There is great hope for the application of Ag-NPs in the versatile field of computers and informatics, cosmetics, textile, food, and medicine. Although a lot of work is done in this field, the full potential of silver nanoparticles is yet to come into lime light with better understanding of their mechanism and long lasting impact on environment and waste management.

9. Chapter summary

The chapter started with a brief introduction of the nanomaterials along with their historical existence without in-depth knowledge. The importance of the silver NPs over other nanometals was established on the account of their properties such as surface-enhanced plasmonic character,

cost, stability, and so on. The synthesis methods and advanced characterization tools were also discussed in keeping AgNPs in the mind. The applications of these competent nanoparticles along with their goodness and special qualities are also described in the chapter. In the end, the challenges and future prospective of this up-bringing area were discussed.

Author details

Neelu Chouhan

Address all correspondence to: niloochauhan@hotmail.com

Department of Pure and Applied Chemistry, University of Kota, Kota, Rajasthan, India

References

[1] Available form: https://www.sciencelearn.org.nz/resources/1676-novel-properties-emerge-at-the-nanoscale

[2] Booker R, Boysen E. Nanotechnology for Dummies. 1st ed. Hoboken NJ: Wiley Publishing; 2005. 40 p. ISBN: 13: 978-0-7645-8368-1

[3] Bonner JT. Why size matters. In: Stevens SY, Sutherland LAM, Krajccik J, editors. The Big Ideas of Nanoscale Science and Engineering. Princeton, NJ: Princeton University Press; 2009. pp. 4-5 (80 p). ISBN 978-1-935155-07-2

[4] Yamamoto M, Nishikawa N, Mayama H, Nonomura Y, Yokojima S, Nakamura S, Uchida K. Theoretical explanation of the lotus effect: Superhydrophobic property changes by removal of nanostructures from the surface of a lotus leaf. Langmuir. 2015;**31**(26):7355-7363. DOI: 10.1021/acs.langmuir.5b00670

[5] Ensikat HJ, Ditsche-Kuru P, Christoph Neinhuis C, Barthlott W. Superhydrophobicity in perfection: The outstanding properties of the lotus leaf. Beilstein J Nanotechnol. 2011;**2**: 152-161. DOI: 10.3762/bjnano.2.19

[6] Koch K, Bhushan B, Barthlott W. Diversity of structure, morphology and wetting of plant surfaces. Soft Matter. 2008;**4**(10):1943-1963. DOI: 10.1039/B804854A

[7] Maier SA. Plasmonics Fundamentals and Applications. 1.st ed. New York: Springer; 2007. pp. 21-34, 65-88. eISBN 978-0387-37825-1

[8] Lal S, Link S, Halas NJ. Nano-optics from sensing to waveguiding. Nature Photonics. 2007;**1**(11):641-648. DOI: 10.1038/nphoton.2007.223

[9] Wang X, Yu JC, Yip HY, Wu L, Wong PK, Lai SY. A mesoporous Pt/TiO$_2$ nanoarchitecture with catalytic and photocatalytic functions. Chemistry – A European Journal. 2005;**11**(10):2997-3004. DOI: 10.1002/chem.200401248

[10] Cao XB, Gu L, Zhuge LJ, Gao WJ, Wang WC, Wu SF. Template-free preparation of hollow Sb2S3 microspheres as supports for Ag nanoparticles and photocatalytic properties of the constructed metal–semiconductor nanostructures. Advanced Functional Materials. 2006;**16**(7):896-902. DOI: 10.1002/adfm.200500422

[11] Virkutyte J, Varma RS. Fabrication and visible light photocatalytic activity of a novel Ag/TiO$_{2-x}$N$_x$ nanocatalyst. New Journal of Chemistry. 2010;**34**(6):1094-1096. DOI: 10.1039/C0NJ00268B

[12] Takagahara T, Takeda K. Theory of the quantum confinement effect on excitons in quantum dots of indirect-gap materials. Physical Review B. 1992;**46**:15578(R). DOI: 10.1103/PhysRevB.46.15578

[13] Couto Jr OD, Puebla J, Chekhovich EA, Luxmoore IJ, Elliott CJ, Babazadeh N, Skolnick MS, Tartakovskii AI, Krysa AB. Charge control in InP/(Ga, In) P single quantum dots embedded in Schottky diodes. Physical Review B. 2011;**84**(12):125301. DOI: 10.1103/PhysRevB.84.125301

[14] Shin SJ, Lee JJ, Kang HJ, Choi JB, Yang SR, Takahashi Y, Hasko DG. Room-temperature charge stability modulated by quantum effects in a nanoscale silicon island. Nano Letters. 2011;**11**(4):1591-1597. DOI: /abs/10.1021/nl1044692

[15] Beenakker CWJ. Theory of Coulomb-blockade oscillations in the conductance of a quantum dot. Physical Review B. 1991;**44**:1646. DOI: 10.1103/PhysRevB.44.1646

[16] Prati E. Valley blockade quantum switching in silicon nanostructures. Journal for Nanoscience and Nanotechnology. 2011;**11**(10):8522-8526. DOI: 10.1166/jnn.2011.4957

[17] Crippa A, Tagliaferri ML, Rotta D, De Michielis M, Mazzeo G, Fanciulli M, Wacquez R, Vinet M, Prati E. Valley blockade and multielectron spin-valley Kondo effect in silicon. Physical Review B. 2015;**92**(3):035424. DOI: 10.1103/PhysRevB.92.035424

[18] Harry A. Atwater, the promise of Plasmonics. Scientific American. 2007;**296**:56-62. DOI: 10.1038/scientificamerican0407-56

[19] Farady M. The Bakerian Lecture: Experimental Relations of Gold (and Other Metals) to Light. Philosophical Transactions of the Royal Society. 1857;**147**:145-181. Bibliography code: 1857RSPT.147.145F

[20] Perrin JB. Nobel Lecture: Discontinuous Structure of Matter. Nobelprize.org. Nobel Media AB 2014. Web. Jan 17, 2018. Available from: http://www.nobelprize.org/nobel_prizes/physics/laureates/1926/perrin-lecture.html

[21] Sharma M, Pathak M, Roy B, Ojha H. Green synthesis of gold nanoparticles using *Cinnamomum verum*, *Syzygium aromaticum* and *Piper nigrum* extract. Asian Journal of Chemistry. 2017;**29**(8):1693-1696. DOI: 10.1007/BF03215599

[22] Ju-Nam Y, Lead JR. Manufactured nanoparticles: An overview of their chemistry, interactions and potential environmental implications. Science of the total environment. 2008;**400**(1):396-414. DOI: 10.1016/j.scitotenv.2008.06.042

[23] McConnell WP, Novak JP, Brousseau LC, Fuierer RR, Tenent RC, Feldheim DL. Electronic and optical properties of chemically modified metal nanoparticles and molecularly bridged nanoparticle arrays. The Journal of Physical Chemistry B. 2000;**104**(38): 8925-8930. DOI: 10.1021/jp000926t

[24] Collier CP, Saykally RJ, Shiang JJ, Henrichs SE, Heath JR. Reversible tuning of silver quantum dot monolayers through the metal-insulator transition. Science. 1997; **277**(5334):1978-1981. DOI: 10.1126/science.277.5334.1978

[25] De M, Ghosh PS, Rotello VM. Applications of nanoparticles in biology. Advanced Materials. 2008;**20**(22):4225-4241. DOI: 10.1002/adma.200703183

[26] Lu AH, Salabas EE, Schüth F. Magnetic nanoparticles: Synthesis, protection, functionalization, and application. Angewandte Chemie International Edition. 2007;**46**(8):1222-1244. DOI: 10.1002/anie.200602866

[27] Ghosh Chaudhuri R, Paria S. Core/shell nanoparticles: Classes, properties, synthesis mechanisms, characterization, and applications. Chemical Reviews. 2011;**112**(4):2373-2433. DOI: 10.1021/cr100449n

[28] Monteiro DR, Gorup LF, Takamiya AS, Ruvollo-Filho AC, de Camargo ER, Barbosa DB. The growing importance of materials that prevent microbial adhesion: Antimicrobial effect of medical devices containing silver. International Journal of Antimicrobial Agents. 2009;**34**(2):103-110. DOI: 10.1016/j.ijantimicag.2009.01.017

[29] Ahamed M, AlSalhi MS, Siddiqui MK. Silver nanoparticle applications and human health. Clinica Chimica Acta. 2010;**411**(23):1841-1848. DOI: 10.1016/j.cca.2010.08.016

[30] García-Barrasa J, López-de-luzuriaga JM, Monge M. Silver nanoparticles on zinc oxide thin film: An insight in fabrication and characterization. Central European Journal of Chemistry. 2011;**64**:9-17. DOI: 10.2478/s11532-010-0124-x

[31] Fabrega J, Luoma SN, Tyler CR, Galloway TS, Lead JR. Silver nanoparticles: Behaviour and effects in the aquatic environment. Environment International. 2011;**37**(2):517-531. DOI: 10.1016/j.envint.2010.10.012

[32] Dallas P, Sharma VK, Zboril R. Silver polymeric nanocomposites as advanced antimicrobial agents: Classification, synthetic paths, applications, and perspectives. Advances in Colloid and Interface Science. 2011;**166**(1):119-135. DOI: 10.1016/j.cis.2011.05.008

[33] Sharma VK, Yngard RA, Lin Y. Silver nanoparticles: Green synthesis and their antimicrobial activities. Advanced Colloidal Interface Science. 2009;**145**:83-96. DOI: 10.1016/j. cis.2008.09.002

[34] Gong HM, Zhou L, Su XR, Xiao S, Liu SD, Wang QQ. Illuminating dark plasmons of silver nanoantenna rings to enhance exciton–plasmon interactions. Advanced Functional Materials. 2009;**19**(2):298-303. DOI: 10.1002/adfm.200801151

[35] Krutyakov YA, Kudrinskiy AA, Olenin AY, Lisichkin GV. Synthesis and properties of silver nanoparticles: Advances and prospects. Russian Chemical Reviews. 2008;**77**(3): 233-257. DOI: 10.1070/RC2008v077n03ABEH003751

[36] West PR, Ishii S, Naik GV, Emani NK, Shalaev VM, Boltasseva A. Searching for better plasmonic devices. Laser & Photonics Reviews. 2000;**2010**:1-13. DOI: 10.1002/lpor.200900055

[37] Oulton RF. Surface plasmon lasers: Sources of nanoscopic light. Materials Today. 2012; **15**(1):26-34. DOI: 10.1016/S1369-7021(12)70018-4

[38] Sharma B, Frontiera RR, Henry AI, Ringe E, Van Duyne RP. SERS: Materials, applications, and the future. Materials Today. 2012;**15**(1):16-25. DOI: 10.1016/S1369-7021(12) 70017-2

[39] Wang P, Huang B, Dai Y, Whangbo MH. Plasmonic photocatalysts: Harvesting visible light with noble metal nanoparticles. Physical Chemistry Chemical Physics. 2012;**14**(28): 9813-9825. DOI: 10.1039/C2CP40823F

[40] Schultz S, Smith DR, Mock JJ, Schultz DA. Single-target molecule detection with nonbleaching multicolor optical immunolabels. Proceedings of the National Academy of Sciences. 2000;**97**(3):996-1001. DOI: 10.1073/pnas.97.3.996

[41] Schultz S, Mock J, Smith DR, Schultz DA. Nanoparticle based biological assays. Journal of Clinical Ligand Assay. 1999;**22**(2):214-216. scholars.duke.edu/display/pub798936

[42] Silva TJ, Schultz S, Weller D. Scanning near-field optical microscope for the imaging of magnetic domains in optically opaque materials. Applied Physics Letters. 1994;**65**(6): 658-660. DOI: 10.1063/1.112261

[43] Sqalli O, Bernal MP, Hoffmann P, Marquis-Weible F. Improved tip performance for scanning near-field optical microscopy by the attachment of a single gold nanoparticle. Applied Physics Letters. 2000;**76**(15):2134-2136. DOI: 10.1063/1.126277

[44] Mie G. Beiträge zur Optik trüber Medien, speziell kolloidaler Metallösungen. Annalen der Physik. 1908;**330**(3):377-445. DOI: 10.1002/andp.19083300302

[45] Sönnichsen C, Franzl T, Wilk T, von Plessen G, Feldmann J, Wilson OV, Mulvaney P. Drastic reduction of plasmon damping in gold nanorods. Physical Review Letters. 2002; **88**(7):077402. DOI: 10.1103/PhysRevLett.88.077402

[46] Valenti M, Dolat D, Biskos G, Schmidt-Ott A, Smith WA. Enhancement of the photoelectrochemical performance of $CuWO_4$ thin films for solar water splitting by plasmonic nanoparticle functionalization. The Journal of Physical Chemistry C. 2015;**119**(4):2096-2104. DOI: 10.1021/jp506349t

[47] Chen HM, Chen CK, Chen CJ, Cheng LC, Wu PC, Cheng BH, Ho YZ, Tseng ML, Hsu YY, Chan TS, Lee JF. Plasmon inducing effects for enhanced photoelectrochemical water splitting: X-ray absorption approach to electronic structures. ACS Nano. 2012;**6**(8):7362-7372. DOI: 10.1021/nn3024877

[48] Erwin WR, Zarick HF, Talbert EM, Bardhan R. Light trapping in mesoporous solar cells with plasmonic nanostructures. Energy & Environmental Science. 2016;**9**(5):1577-1601. DOI: 10.1039/C5EE03847B

[49] Piot A, Earl SK, Ng C, Dligatch S, Roberts A, Davis TJ, Gómez DE. Collective excitation of plasmonic hot-spots for enhanced hot charge carrier transfer in metal/semiconductor contacts. Nanoscale. 2015;**7**(18):8294-8298. DOI: 10.1039/C5NR01592H

[50] Li J, Cushing SK, Zheng P, Meng F, Chu D, Wu N. Plasmon-induced photonic and energy-transfer enhancement of solar water splitting by a hematite nanorod array. Nature Communications. 2013;**4**:2651. DOI: 10.1038/ncomms3651

[51] Linic S, Christopher P, Ingram DB. Plasmonic-metal nanostructures for efficient conversion of solar to chemical energy. Nature Materials. 2011;**10**(12):911-921. DOI: 10.1038/nmat3151

[52] Cushing SK, Wu N. Progress and perspectives of plasmon-enhanced solar energy conversion. The Journal of Physical Chemistry Letters. 2016;**7**(4):666-675. DOI: 10.1021/acs.jpclett.5b02393

[53] Haro M, Abargues R, Herraiz-Cardona I, Martínez-Pastor J, Giménez S. Plasmonic versus catalytic effect of gold nanoparticles on mesoporous TiO_2 electrodes for water splitting. Electrochimica Acta. 2014;**144**:64-70. DOI: 10.1016/j.electacta.2014.07.146

[54] Quinten M. Optical Properties of Nanoparticle Systems. Wiley-VCH Verlag GmbH & Co. KGaA; Weinheim, Germany, 2011. pp. 55-74. ISBN: 978-3-527-41043-9

[55] Pathak NK, Pandey GK, Ji A, Sharma RP. Study of light extinction and surface plasmon resonances of metal nanocluster: A comparison between coated and non-coated nanogeometry. Plasmonics. 2015;**10**(6):1597-1606. DOI: 10.1007/s11468-015-9978-2

[56] Huang X, El-Sayed IH, Qian W, El-Sayed MA. Cancer cell imaging and photothermal therapy in the near-infrared region by using gold nanorods. Journal of the American Chemical Society. 2006;**128**(6):2115-2120. DOI: 10.1021/ja057254a

[57] Kadkhodazadeh S, de Lasson JR, Beleggia M, Kneipp H, Wagner JB, Kneipp K. Scaling of the surface plasmon resonance in gold and silver dimers probed by EELS. The Journal of Physical Chemistry C. 2014;**118**(10):5478-5485. DOI: 1021 jp500288s

[58] Nordlander P, Oubre C, Prodan E, Li K, Stockman MI. Plasmon hybridization in nanoparticle dimers. Nano Letters. 2004;**4**(5):899-903. DOI: 10.1021/nl049681c

[59] Jain PK, Huang W, El-Sayed MA. On the universal scaling behavior of the distance decay of plasmon coupling in metal nanoparticle pairs: A plasmon ruler equation. Nano Letters. 2007;**7**(7):2080-2088. DOI: 10.1021/nl071008a

[60] Quinten M, Leitner A, Krenn JR, Aussenegg FR. Electromagnetic energy transport via linear chains of silver nanoparticles. Optics Letters. 1998;**23**(17):1331-1333. DOI: 10.1364/OL.23.001331

[61] Stiles PL, Dieringer JA, Shah NC, Van Duyne RP. Surface-enhanced Raman spectroscopy. Annual Review of Analytical Chemistry. 2008;**1**:601-626. DOI: 10.1146/annurev.anchem.1.031207.112814

[62] Belkin M, Chao SH, Jonsson MP, Dekker C, Aksimentiev A. Plasmonic nanopores for trapping, controlling displacement, and sequencing of DNA. ACS Nano. 2015;**9**(11):10598-10611. DOI: 10.1021/acsnano.5b0417

[63] Zhang L, Herrmann LO, Baumberg JJ. Size dependent plasmonic effect on $BiVO_4$ photoanodes for solar water splitting. Scientific Reports. 2015;**5**:16660. DOI: 10.1038/srep16660

[64] Callahan DM, Munday JN, Atwater HA. Solar cell light trapping beyond the ray optic limit. Nano letters. 2012;**12**(1):214-218. DOI: 10.1021/nl203351k

[65] Kelly KL, Coronado E, Zhao LL, Schatz GC. The optical properties of metal nanoparticles: The influence of size, shape, and dielectric environment. Journal of Physical Chemistry B. 2002;**107**:668-677. DOI: 10.1021/jp026731y

[66] Atwater HA, Polman A. Plasmonics for improved photovoltaic devices. Nature Materials. 2010;**9**(3):205-213. DOI: 10.1038/nmat2629

[67] Mtangi W, Tassinari F, Vankayala K, Vargas Jentzsch A, Adelizzi B, Palmans AR, Fontanesi C, Meijer EW, Naaman R. Control of electrons' spin eliminates hydrogen peroxide formation during water splitting. Journal of the American Chemical Society. 2017;**139**(7):2794-2798. DOI: 10.1021/jacs.6b12971

[68] Valenti M, Jonsson MP, Biskos G, Schmidt-Otta A, Smith WA. Plasmonic nanoparticle – semiconductor composites for efficient solar water splitting. Journal of Materials Chemistry A. 2016;**4**:17891-17912. DOI: 10.1039/c6ta06405a

[69] Rauwel P, Rauwel E, Ferdov S, Singh MP. Chapter 1: Silver Nanoparticles: Synthesis, Properties, and Applications in the book Advances in Materials Science and Engineering. 2015. pp. 624394 (2 pages). DOI: 10.1155/2015/624394

[70] Jin R, Cao Y, Mirkin CA, Kelly KL, Schatz GC, Zheng JG. Photoinduced conversion of silver nanospheres to nanoprisms. Science. 2001;**294**(5548):1901-1903. DOI: 10.1126/science.1066541

[71] Jin R, Cao YC, Hao E, Metraux GS, Schatz GC, Mirkin CA. Controlling anisotropic nanoparticle growth through plasmon excitation. Nature. 2003;**425**:487-490. DOI: 10.1038/nature02020

[72] Hao E, Kelly KL, Hupp JT, Schatz GC. Synthesis of silver nanodisks using polystyrene mesospheres as templates. Journal of the American Chemical Society. 2002;**124**(51): 15182-15183. DOI: 10.1021/ja028336r

[73] Pastoriza-Santos I, Liz-Marzon LM. Synthesis of silver nanoprisms in DMF. Nano Letters. 2002;**2**:903-905. DOI: 10.1021/nl025638i

[74] Wang L, Chen X, Zhan J, Chai Y, Yang C, Xu L, Zhuang W, Jing B. Synthesis of gold nano-and microplates in hexagonal liquid crystals. The Journal of Physical Chemistry B. 2005;**109**(8):3189-3194. DOI: 10.1021/jp0449152

[75] Kim JU, Cha SH, Shin K, Jho JY, Lee JC. Preparation of gold nanowires and nanosheets in bulk block copolymer phases under mild conditions. Advanced Materials. 2004;**16**(5): 459-464. DOI: 10.1002/adma.200305613

[76] Shao Y, Jin Y, Dong S. Synthesis of gold nanoplates by aspartate reduction of gold chloride. Chemical Communications. 2004;**9**:1104-1105. DOI: 10.1039/B315732F

[77] Sarma TK, Chattopadhyay A. Starch-mediated shape-selective synthesis of au nanoparticles with tunable longitudinal plasmon resonance. Langmuir. 2004;**20**(9):3520-3524. DOI: 10.10 21/la049970g

[78] Pal T, Maity DS, Ganguly A. Use of a silver-gelatin complex for the determination of micro-amounts of hydrazine in water. The Analyst. 1986;**111**(12):1413-1415. DOI: 10.1039/ AN9861101413

[79] Link S, Wang ZL, El-Sayed MA. Alloy formation of gold-silver nanoparticles and the dependence of the plasmon absorption on their composition. The Journal of Physical Chemistry B. 1999;**103**(18):3529-3533. DOI: 10.1021/jp990387w

[80] Pastoriza-Santos I, Liz-Marzán LM. Formation of PVP-protected metal nanoparticles in DMF. Langmuir. 2002;**18**(7):2888-2894. DOI: 10.1021/la015578g

[81] Fievet F, Lagier JP, Figlarz M. Preparing monodisperse metal powders in micrometer and submicrometer sizes by the polyol process. MRS Bulletin. 1989;**12**:29-34. DOI: 10. 1557/S0883769400060930

[82] Yamamoto T, Wada Y, Sakata T, Mori H, Goto M, Hibino S, Yanagida S. Microwave-assisted preparation of silver nanoparticles. Chemistry Letters. 2004;**33**(2):158-159. DOI: 10.1246/cl.2004.158

[83] Chou KS, Ren CY. Synthesis of nanosized silver particles by chemical reduction method. Materials Chemistry and Physics. 2000;**64**(3):241-246. DOI: 10.1016/S0254-0584(00)00223-6

[84] Chen SF, Zhang H. Aggregation kinetics of nanosilver in different water conditions. Advances in Natural Sciences: Nanoscience and Nanotechnology. 2012;**3**(3):035006. DOI: 10.1088/2043-6262/3/3/035006/meta

[85] Dang TM, Le TT, Fribourg-Blanc E, Dang MC. Influence of surfactant on the preparation of silver nanoparticles by polyol method. Advances in Natural Sciences: Nanoscience and Nanotechnology. 2012;**3**(3):035004. DOI: 10.1088/2043-6262/3/3/035004/meta

[86] Patil RS, Kokate MR, Jambhale CL, Pawar SM, Han SH, Kolekar SS. One-pot synthesis of PVA-capped silver nanoparticles their characterization and biomedical application. Advances in Natural Sciences: Nanoscience and Nanotechnology. 2012;**3**(1):015013. DOI: 10.1088/2043-6262/3/1/015013/meta

[87] Henglein A. Physicochemical properties of small metal particles in solution: "microelectrode" reactions, chemisorption, composite metal particles, and the atom-to-metal transition. The Journal of Physical Chemistry. 1993;**97**(21):5457-5471. DOI: 10.1021/j100123a004

[88] Pastoriza-Santos I, Liz-Marzán LM. Synthesis of silver nanoprisms in DMF. Nano Letters. 2002;**2**(8):903-905. DOI: 10.1021/nl025638i

[89] Lu W, Liao F, Luo Y, Chang G, Sun X. Hydrothermal synthesis of well-stable silver nanoparticles and their application for enzymeless hydrogen peroxide detection. Electrochimica Acta. 2011;**56**(5):2295-2298. DOI: 10.1016/j.electacta.2010.11.053

[90] Lee DK, Kang YS. Synthesis of silver nanocrystallites by a new thermal decomposition method and their characterization. ETRI Journal. 2004;**26**(3):252-256. DOI: HJTODO_2004_v26n3_252

[91] Jung JH, Oh HC, Noh HS, Ji JH, Kim SS. Metal nanoparticle generation using a small ceramic heater with a local heating area. Journal of Aerosol Science. 2006;**37**(12):1662-1670. DOI: 10.1016/j.jaerosci.2006.09.002

[92] Tien DC, Tseng KH, Liao CY, Huang JC, Tsung TT. Discovery of ionic silver in silver nanoparticle suspension fabricated by arc discharge method. Journal of Alloys and Compounds. 2008;**463**(1):408-411. DOI: 10.1016/j.jallcom.2007.09.048

[93] Siegel J, Kvítek O, Ulbrich P, Kolská Z, Slepička P and Švorčík V. Progressive approach for metal nanoparticle synthesis. Materials Letters. 2012;**89**:47-50. DOI: 10.1016/j.matlet.2012.08.048

[94] Sakamoto M, Fujistuka M, Majima T. Light as a construction tool of metal nanoparticles: Synthesis and mechanism. Journal of Photochemistry and Photobiology C: Photochemistry Reviews. 2009;**10**(1):33-56. DOI: 10.1016/j.jphotochemrev.2008.11.002

[95] Christy AJ, Umadevi M. Synthesis and characterization of monodispersed silver nanoparticles. Advances in Natural Sciences: Nanoscience and Nanotechnology. 2012;**3**(3):035013. DOI: 10.1088/2043-6262/3/3/035013/meta

[96] Sato-Berrú R, Redón R, Vázquez-Olmos A, Saniger JM. Silver nanoparticles synthesized by direct photoreduction of metal salts. Application in surface-enhanced Raman spectroscopy. Journal of Raman Spectroscopy. 2009;**40**(4):376-380. DOI: 10.1002/jrs.2135

[97] Ghosh SK, Kundu S, Mandal M, Nath S, Pal T. Studies on the evolution of silver nanoparticles in micelle by UV-photoactivation. Journal of Nanoparticle Research. 2003;**5**(5–6):577-587. DOI: 10.1023/B:NANO.0000006100.25744.fa

[98] Huang L, Zhai ML, Long DW, Peng J, Xu L, Wu GZ, Li JQ, Wei GS. UV-induced synthesis, characterization and formation mechanism of silver nanoparticles in alkalic carboxymethylated chitosan solution. Journal of Nanoparticle Research. 2008;**10**(7):1193-1202. DOI: 10.1007/s11051-007-9353-0

[99] Sakamoto M, Fujistuka M, Majima T. Light as a construction tool of metal nanoparticles: Synthesis and mechanism. Journal of Photochemistry and Photobiology C: Photochemistry Reviews 2009;**10**(1):33-56. DOI: 10.1016/j.jphotochemrev.2008.11.002

[100] Tang B, Sun L, Li JL, Zhang M, Wang X. Sunlight-driven synthesis of anisotropic silver nanoparticles. Chemical Engineering Journal. 2015;**260**:99-106. DOI: 10.1016/j.cej.2014.08.044

[101] Chouhan N, Ameta R, Meena RK. Biogenic silver nanoparticles from Trachyspermum ammi (Ajwain) seeds extract for catalytic reduction of p-nitrophenol to p-aminophenol in excess of NaBH$_4$. Journal of Molecular Liquids. 2017;**230**:74-84. DOI: 10.1016/j.molliq.2017.01.003

[102] Roy N, Gaur A, Jain A, Bhattacharya S, Rani V. Green synthesis of silver nanoparticles: An approach to overcome toxicity. Environmental Toxicology and Pharmacology. 2013; **36**(3):807-812. DOI: 10.1016/j.etap.2013.07.005

[103] Thakkar KN, Mhatre SS, Parikh RY. Biological synthesis of metallic nanoparticles. Nanomedicine: Nanotechnology, Biology and Medicine. 2010;**6**(2):257-262. DOI: 10.1016/j.nano.2009.07.002

[104] Scherrer P. Bestimmung der Größe und der inneren Struktur von Kolloidteilchen mittels Röntgenstrahlen. Nachrichten von der Gesellschaft der Wissenschaften zu Göttingen. Mathematisch-Physikalische Klasse. 1918;**1918**:98-100. DOI: eudml.org/doc/59018

[105] Wiley B, Sun YG, Xia YN. Synthesis of silver nanostructures with controlled shapes and properties. Accounts of Chemical Research. 2007;**40**:1067-1076. DOI: 10.1021/ar7000974

[106] Liang H. Rossouw D, Zhao H, Cushing SK, Shi H, Korinek A, Xu H, Rosei F, Wang W, Wu N, Botton GA, Ma D. Asymmetric silver "Nanocarrot" structures: Solution synthesis and their asymmetric plasmonic resonances. Journal of the American Chemical Society. 2013;**135**:9616-9619. DOI: 10.1021/ja404345s

[107] Miles MJ, Master T. Mc, HJ, Lambert N, Scanning tunneling microscopy of biomolecules. Journal of Vacuum Science & Technology A: Vacuum Surfaces and Films. 1990;**8**(1):698-702. DOI: 10.1116/1.576986

[108] Chi L, Röthig C. Scanning probe microscopy of nanoclusters. In: Wang ZL, editor. Characterization of Nanophase Materials. Weinheim, Germany: Wiley-VCH, Verlag GmbH; 2000:133-163. DOI: 10.1002/3527600094.ch5

[109] Gmoshinski IV, Khotimchenko SA, Popov VO, Dzantiev BB, Zherdev AV, Demin VF, Buzulukov YP. Nanomaterials and nanotechnologies: Methods of analysis and control. Russian Chemical Reviews. 2013;**82**(1):48. DOI: 10.1070/RC2013v082n01ABEH004329/meta

[110] Tiede K, Boxall ABA, Tear SP, Lewis J, David H, Hassellöv M. Detection and characterization of engineered nanoparticles in food and the environment. Food Additives & Contaminants: Part A. 2008;**25**:795-821. DOI: 10.1080/02652030802007553

[111] Schmidt FP, Ditlbacher H, Hohenester U, Hohenau A, Hofer F, Krenn JR. Universal dispersion of surface plasmons in flat nanostructures. Nature Communications. 2014;**5**: 3604. DOI: 10.1038/ncomms4604

[112] Nicoletti O, de La Peña F, Leary RK, Holland DJ, Ducati C, Midgley PA. Three-dimensional imaging of localized surface plasmon resonances of metal nanoparticles. Nature. 2013;**502**(7469):80-84. DOI: 10.1038/nature12469

[113] Schmidt FP, Ditlbacher H, Hohenester U, Hohenau A, Hofer F, Krenn JR. Dark plasmonic breathing modes in silver nanodisks. Nano Letters. 2012;**12**(11):5780-5783. DOI: 10.1021/nl3030938

[114] Guiton BS, Iberi V, Li S, Leonard DN, Parish CM, Kotula PG, Varela M, Schatz GC, Pennycook SJ, Jon P. Camden correlated optical measurements and plasmon mapping of silver nanorods. Nano Letters. 2011;**11**(8):3482-3488. DOI: 10.1021/nl202027h

[115] Mock JJ, Barbic M, Smith DR, Schultz DA, Schultz S. Shape effects in plasmon resonance of individualcolloidal silver nanoparticles. The Journal of Chemical Physics. 2002; **116**(15):6755-6759. DOI: 10.1063/1.1462610

[116] Baia L, Simon S. UV-VIS and TEM assessment of morphological features of silver nanoparticles from phosphate glass matrices. In: Méndez-Vilas A, Díaz J, editors. Modern Research and Educational Topics in Microscopy. 2007:576-583. DOI: 10.1.1.605.2338

[117] Seney CS, Gutzman BM, Goddard RH. Correlation of size and surface-enhanced Raman scattering activity of optical and spectroscopic properties for silver nanoparticles. The Journal of Physical Chemistry C. 2008;**113**(1):74-80. DOI: 10.1021/jp805698e

[118] Liang H, Li Z, Wang Z, Wang W, Rosei F, Ma D, Xu H. Enormous surface-enhanced raman scattering from dimers of flower-like silver mesoparticles. Small. 2012;**8**(22):3400-3405. DOI: 10.1002/smll.201201081

[119] Butun S, Sahiner N. A versatile hydrogel template for metal nano particle preparation and their use in catalysis. Polymer. 2011;**52**(21):4834-4840. DOI: 10.1016/j.polymer.2011.08.021

[120] Harish S, Sabarinathan R, Joseph J, Phani KL. Role of pH in the synthesis of 3-aminopropyl trimethoxysilane stabilized colloidal gold/silver and their alloy sols and their application to catalysis. Materials Chemistry and Physics. 2011;**127**(1):203-207. DOI: 10.1016/j.matchemphys.2011.01.060

[121] Cao Y, Li D, Jiang F, Yang Y, Huang Z. Engineering metal nanostructure for SERS application. Journal of Nanomaterials. 2013;**2013**:01-12. DOI: 10.1155/2013/123812

[122] Botta R, Upender G, Sathyavathi R, Rao DN, Bansal C. Silver nanoclusters films for single molecule detection using surface enhanced Raman scattering (SERS). Materials Chemistry and Physics. 2013;**137**(3):699-703. DOI: 10.1016/j.matchemphys.2012.10.022

[123] Zhu SQ, Zhang T, Guo XL, Wang QL, Liu X, Zhang XY. Gold nanoparticle thin films fabricated by electrophoretic deposition method for highly sensitive SERS application. Nanoscale Research Letters. 2012;**7**(1):613. DOI: 10.1186/1556-276X-7-613

[124] Rauwel P, Rauwel E, Ferdov S, Singh MP. Silver nanoparticles: Synthesis, properties, and applications. Advances in Materials Science and Engineering. 2015;**2015**:624394 (2 p). DOI: 10.1155/2015/624394

[125] Zhang T, Song YJ, Zhang XY, Wu JY. Synthesis of silver nanostructures by multistep methods. Sensors. 2014;**14**:5860-5889. DOI: 10.3390/s140405860

[126] Fauss E. The Silver Nanotechnology Commercial Inventory. Charlottesville, VA: University of Virginia; 2008. Available from: http://www.nanoproject.org

[127] Alivisatos P. The use of nanocrystals in biological detection. Nature Biotechnology. 2004; **22**(1):47-52. DOI: 10.1038/nbt927

[128] Hong Y, Huh YM, Yoon DS, Yang J. Nanobiosensors based on localized surface plasmon resonance for biomarker detection. Journal of Nanomaterials. 2012;**2012**:111. DOI: 10.1155/2012/759830

[129] Tripp RA, Dluhy RA, Zhao Y. Novel nanostructures for SERS biosensing. Nano Today. 2008;**3**(3):31-37. DOI: 10.1016/S1748-0132(08)70042-2

[130] Samanta A, Maiti KK, Soh KS, Liao X, Vendrell M, Dinish US, Yun SW, Bhuvaneswari R, Kim H, Rautela S, Chung J. Ultrasensitive near-infrared Raman reporters for SERS-based in vivo cancer detection. Angewandte Chemie International Edition. 2011;**50**(27):6089-6092. DOI: 10.1002/anie.201007841

[131] Kumar A, Boruah BM, Liang XJ. Gold nanoparticles: Promising nanomaterials for the diagnosis of cancer and HIV/AIDS. Journal of Nanomaterials. 2011;**2011**:22. DOI: 10.1155/2011/202187

[132] Atwater HA. The promise of plasmonics. Scientific American. 2007;**296**(4):56-62. DOI: 10.1038/scientificamerican0407-56

[133] Brennan SA, Ní Fhoghlú C, Devitt BM, O'Mahony FJ, Brabazon D, Walsh A. Silver nanoparticles and their orthopaedic applications. Bone & Joint Journal. 2015;**97-B**:582-589. DOI: 10.1302/0301-620X.97B5.33336

[134] ZhiLiang J, Yuan C, AiHui L, HuiLin T, NingLi T, FuXin Z. Silver nanoparticle labeled immunoresonance scattering spectral assay for trace fibrinogen. Science in China Series B. 2007;**50**:345-350. DOI: 10.1007/s11426-007-0064-2

[135] Dong XY, Gao ZW, Yang KF, Zhang WQ, Xu LW. Nanosilver as a new generation of silver catalysts in organic transformations for efficient synthesis of fine chemicals. Catalysis Science & Technology. 2015;**5**(5):2554-2574. DOI: 10.1039/C5CY00285K

[136] Chouhan N, Ameta R, Meena RK. Biogenic silver nanoparticles from Trachyspermum ammi (Ajwain) seeds extract for catalytic reduction of p-nitrophenol to p-aminophenol in excess of NaBH$_4$. Journal of Molecular Liquids. 2017;**230**:74-84. DOI: 10.1016/j.molliq.2017.01.003

[137] Bhosale MA, Bhanage BM. Silver nanoparticles: Synthesis, characterization and their application as a sustainable catalyst for organic transformations. Current Organic Chemistry. 2015;**19**(8):708-727. DOI: 10.2174/1385272819666150207001154

[138] Yoon KY, Byeon JH, Park CW, Hwang J. Antimicrobial effect of silver particles on bacterial contamination of activated carbon fibers. Environmental Science & Technology. 2008;**42**(4):1251-1255. DOI: 10.1021/es0720199

[139] Hongyin Z. Application of Silver Nanoparticles in Drinking Water Purification. 2013. Open Access Dissertations. Paper 29. DOI: http://digitalcommons.uri.edu/oa_diss/29

[140] Rai M, Birla S, Ingle A, et al. Nanosilver: An inorganic nanoparticle with myriad potential applications. Nanotechnology Reviews. 2014;**3**(3):281-309. DOI: 10.1515/ntrev-2014-0001

[141] Holladay RJ. Toothpaste or tooth gel containing silver nanoparticles coated with silver oxide. US 20130017236 A1

[142] Ha TH, Jeong JY, Jung BH, Kim JK, Lim YT, Cosmetic pigment composition containing gold or silver nano-particles. WO 2007011103 A1

[143] Zhao Z, Zhang B, Lin K. Nano-silver antibacterial liquid soap and preparation method thereof. CN102860923 B

[144] Nia JR. Nanosilver for preservation and treatment of diseases in agriculture field. US 0075818 A1

[145] Zhang G, Liu Y, Gao X, Chen Y. Synthesis of silver nanoparticles and antibacterial property of silk fabrics treated by silver nanoparticles. Nanoscale Research Letters. 2014;**9**:216-223. DOI: 10.1186/1556-276X-9-216

[146] Montazer M, Hajimirzababa H, Rahimi MK, Alibakhshi S. Durable anti-bacterial nylon carpet using colloidal nano silver. Fibres & Textiles in Eastern Europe. 2012;**4**(93):96-101. DOI: http://www.fibtex.lodz.pl/article757.html

[147] Nel A, Xia T, Mädler L, Li N. Toxic potential of materials at the nanolevel. Science. 2006; **311**(5761):622-627. DOI: 10.1126/science.1114397

[148] Levard C, Hotze EM, Lowry GV, Brown Jr GE. Environmental transformations of silver nanoparticles: Impact on stability and toxicity. Environmental Science & Technology. 2012;**46**(13):6900-6914. DOI: 10.1021/es2037405

[149] Wu K, Chen J, McBride JR, Lian T. Efficient hot-electron transfer by a plasmon-induced interfacial charge-transfer transition. Science. 2015;**349**:632-635. DOI: 10.1126/science. aac5443

[150] Kumarasinghe CS, Premaratne M, Bao Q, Agrawal GP. Theoretical analysis of hot electron dynamics in nanorods. Scientific Reports. 2015;**5**:12140. DOI: 10.1038/srep12140

[151] Harutyunyan H, Martinson AB, Rosenmann D, et al. Anomalous ultrafast dynamics of hot plasmonic electrons in nanostructures with hot spots. Nature Nanotechnology. 2015; **10**:770-774. DOI: 10.1038/nnano.2015.165

[152] Saavedra JR, Asenjo-Garcia A, García de Abajo FJ. Hot-electron dynamics and thermalization in small metallic nanoparticles. ACS Photonics. 2016;**3**(9):1637-1646. DOI: 10.1021/ acsphotonics.6b00217

[153] Méjard R, Verdy A, Petit M, Bouhelier A, Cluzel B, Demichel O. Energy-resolved hot-carrier relaxation dynamics in monocrystalline plasmonic nanoantennas. ACS Photonics. 2016;**3**(8):1482-1488. DOI: 10.1021/acsphotonics.6b00033